Feasibility and applications of non-invasive laser photogrammetry on free-ranging coastal dolphins

A thesis presented for the degree of Bachelor of Science with Honours in Marine Science. School of Veterinary & Life Sciences, Murdoch University,

Western Australia

Martin van Aswegen BSc

May 2017

Declaration

I declare that this thesis is my own account of my research and contains as its main content, work, which has not previously been submitted for a degree at any other tertiary education institution.

…….

Martin van Aswegen

Abstract

Morphometric data plays a pivotal role in understanding key life history traits to elucidate biological, ecological and evolutionary processes. Obtaining morphometric data from free-ranging cetaceans is difficult, as traditional methods rely on either post-mortem or highly-invasive techniques. The present study evaluated the feasibility of remote laser photogrammetry as a non-invasive technique to obtain morphometric data on free-ranging coastal dolphins. First, simulation models and post-mortem specimens were used to investigate potential sources of measurement error and quantify their influence on the accuracy and precision of the morphometric data. These sources include horizontal angle, distance, and body curvature. Second, to demonstrate the potential applications of this technique, laser photogrammetry measurements were obtained during boat-based photo-identification surveys on Indo-Pacific bottlenose dolphins (*Tursiops aduncus*) from Western Australia (Bunbury, Shark Bay and Mandurah). Laser-derived, blowhole-to-dorsal fin (BH-DF) measurements were obtained from individuals of known ages in Bunbury (*N*=103) and Shark Bay (*N*=76), in addition to individuals in Mandurah (*N*=28). Our laser-derived measurement data facilitated the development of population growth curves in conjunction with longitudinal demographic data from Bunbury (~10 years) and Shark Bay (~33 years). These growth curves characterise not only the relationship between age and length, but also the significant morphological differences between these geographically-isolated populations. This study demonstrates the value of remote laser photogrammetry as an effective tool to investigate individual and population-based growth and life-history parameters. This non-invasive technique will provide unique opportunities to better understand the ecological, demographic and life-history characteristics of a population and so better inform conservation management strategies for free-ranging cetacean populations.

Contents

List of Tables

List of Figures

Figure 3.1 Plot exhibiting the results of the two-dimensional experiment, where horizontal angle was tested from 0° to 75°, using five distance increments (5-25m). Note the region of low measurement error at horizontal angles less than ~20°.

Figure 3.2 Relationship between total body length and the distance between blowhole and dorsal fin for Indo-Pacific bottlenose dolphins (N=10). The black line represents the fitted line of a linear model (TBL= 3.16 X BH-DF).

Figure 3.3 Age-frequency distributions of male (□), female (■) and unknown sex (■) T. aduncus sampled in Bunbury (A), Shark Bay (B) and Mandurah (C). Age bins represent the three years prior to the bin in question, e.g. the '3' age bin represents years 1 to 3.

Figure 3.4 Visual representation of each of the model fits (see legends) relative to the length-at-age data obtained for each population (Bunbury, **A**, N = 103; Shark Bay, **B**, N = 75; Mandurah, **C**, N = 28).

Figure 3.5 Combined-sex Richards growth curves (—) for T. aduncus sampled in Bunbury, Shark Bay and Mandurah study sites. Male (△), female (□), and unknown sex (○) dolphins are plotted, along with sub-setted male (- -) and female (- -) lines. Reference lines (- -) have been added to highlight the inflection point at various years of age: 1, 3 (weaning) and 12 (age at maturity).

Figure 3.6 Visual representations of the bootstrapped error distributions characterising the relative measurement and age estimation error associated with each individual sampled in Bunbury **(A)** and Shark Bay **(B)**. Bootstrapped RGF curves are also displayed in red. Note the increased size of the error distributions for mature Bunbury individuals with relatively less error present in younger individuals.

Figure 3.7 Frequency distributions representing the density distributions around the bootstrapped length-at-age values between Bunbury and Shark Bay. Differences in blowhole-to-dorsal fin length (BH-DF) were tested using four age classes: years 1, 3, 12, and 25.

Figure 3.8 Bootstrapped density distributions of parameter values of the RGF growth model fitted to length -at -age data from Bunbury (blue) and Shark Bay (grey) individuals across the four tested age classes. Note the significant differences in BH-DF length demonstrated by a lack of overlapping distributions.

Figure 3.9 Overlaid RGF curves for Bunbury (—) and Shark Bay (—) demonstrating the differences in length-at-age measurements of sampled individuals. Note the lack of overlapping data points between the two populations.

Acknowledgements

Firstly, thank you to Professor Lars Bejder for giving me this opportunity, it has been a learning experience but I have thoroughly enjoyed the journey.

Thank you to my supervisors Professor Lars Bejder and Dr. Fredrik Christiansen for your mentoring and direction throughout the year, it was such a pleasure to work with you both.

I would like to thank John Symons, Krista Nicholson, Valeria Senigaglia, Delphine Chabanne and Caitlin Karniski for the awesome memories and for allowing me to collect as much data as possible out in the field. The dolphins did not always make it easy, so your patience was truly appreciated.

A big thank you to all the volunteers in Bunbury, Mandurah and Shark Bay who helped me throughout the year – not only for your assistance but also for all the good times and laughs.

Thank you to Nahiid Stephens for letting me participate in several dolphin necropsies and for allowing me to use the lasers on the post-mortem dolphins, it made a huge difference!

Thank you to Jan Tierney and Linda for sharing all your local knowledge on the Bunbury dolphins and their respective histories.

I must thank Sally and Harry Kirby for everything they have done for me over the years, your support is truly appreciated.

A big thank you to my girlfriend Hannah for all your support, wisdom and late night skypes.

Finally, I would like to say a special thank you to my family for the relentless support and understanding they have provided me over the last year.

1. Introduction

A comprehensive understanding of population-specific demographics, life history traits and behavioural ecology is essential for the effective management of animal populations. Many life history and reproductive dynamics are linked to morphological and age-specific processes, which, in turn, can be affected by biological, social, ecological and anthropogenic factors (Panik, 2014). This type of data serves as the basis for characterising individual and population-level dynamics and is useful in establishing species or population vulnerability and recovery-potential (Olsen *et al*., 2014). However, obtaining representative morphological and demographic data for free-ranging species has proven to be problematic, as reflected by a notable deficiency of such data for several marine vertebrate species (Peltier *et al*., 2012). Traditionally and currently, an inherent reliance on classic approaches is evident, typically comprising of post-mortem investigations or highly invasive techniques, such as the physical capture and release of free-ranging small dolphins. Hence, it is necessary to examine how these data may be collected *in situ*. This thesis introduces laser photogrammetry as an alternative means of collecting morphological data, with an emphasis placed on the feasibility and applicability of this emerging non-invasive technique. I will demonstrate a variety of applications of morphometric and age-specific data on marine vertebrates, and will provide a revision of the accepted techniques to collect this type of information. The merits of pertinent morphometric and age estimation techniques will be evaluated and our sustained reliance on post-mortem and invasive techniques in the past illustrated, highlighting the need for alternative non-invasive sampling techniques

1.1 The role of morphometric data within wildlife biology

Morphometry is a form of quantitative analysis which investigates the external shape and dimensions of objects or living organisms through the collection of length, angle, surface and volumetric measurements (Zelditch *et al.*, 1952). The broad field of morphometry provides a diverse range of applications relating to the biology, ecology and evolution of fauna (Blackwell, Bassett & Dickman, 2006). The following sections describe the role that morphometric data have within numerous applications and provide examples of how morphology may be used to investigate life history (physical and sexual maturity), demographic and taxonomic characteristics of free-ranging cetacean populations.

Understanding the life-history traits of cetaceans by utilising length and mass is a valuable approach. For example, the onset of sexual maturity in delphinids has been assessed extensively using gonadal size and weight, the degree of cranial fusion in both immature and mature skulls as well as external length measurements (Van Waerebeek, 1993; Galatius *et al*., 2011; Jefferson *et al*., 2002; Kemper *et al*., 2014; Jordan *et al*., 2015). By establishing life-history parameters for both intra- and inter-specific population comparisons, biologists can better understand the local adaptations and reproductive potential of populations, thereby allowing more accurate assessment of a population's vulnerability to anthropogenic pressures or natural changes in their environment.

Morphometric data are pivotal in determining the physical condition of both live and deceased marine mammals and can be quantified by employing one or more applicable indices (Christiansen *et al*., 2016). For example, morphometric indices (e.g. blubber thickness, muscle/blubber trunk mass ratio as well as body girth and width) are considered reliable indicators of nutritional condition (Hart *et al*., 2013), as an organism's energy reserves are stored generally as lipids within blubber adipocytes or fat cells (Goméz-Campos *et al*., 2011). Body condition can fluctuate in response to prey availability and consumption

(Auttila *et al*., 2016), pathology (Wang *et al*., 2007) and external factors relating to reproductive processes and predator avoidance (Heithaus & Dill, 2002; Fearnbach *et al*., 2011). Recently, Christiansen *et al*. (2016) demonstrated the importance of specific nursery grounds by quantifying the energy transfer from lactating humpback whale (*Megaptera novaeangliae*) females to their calves. Surface area measurements showed that mothers were losing approximately 1 cm of girth every few days in preparing their calves for the southern migration to Antarctica. Such data allow researchers to explore and identify key processes relating to body condition in order to determine survival and reproductive success rates, which are pivotal for the establishment of effective population management strategies.

Morphometric data can also be used to characterise and distinguish individuals amongst and between animal groups. Sexual dimorphism serves as a classic example in which sexes can be distinguished through morphological differences. In cetaceans, sexual dimorphism can be determined using total length as in the case for sperm whales (*Physeter macrocephalus*; Cranford, 1999), secondary characteristics such as the dorsal fin shape and height for killer whales (*Orcinus orca*; Durban & Parsons, 2006), as well as contrasting colouration patterns such as ventral speckling (Krzyszczyk & Mann, 2012) and dorsal fin pigmentation (Brown *et al*., 2016). A host of morphological measurements have been utilised to explain differing physiological and biological characteristics between intra-specific populations and subspecies, generally revolving around external body and limb measurements, life-history parameters and internal osteological characteristics (Baker *et al*., 2002; Chen *et al*., 2011). Similar measurements have been applied to many taxonomic groups including marine and terrestrial invertebrates (Tofilski, 2000), reptiles (Klutsch *et al*., 2007), fish (Trabelsi *et al*., 2004) and mammals (Baker *et al*., 2002; Charlton-Robb *et al*., 2011; Groeneveld *et al*., 2011; del Castillo *et al*., 2014). These differences can be attributed to ontogenetic allometry (Bilgmann *et al*., 2007), genetic differences (Hale *et al*., 2000) and ecological factors

(Monteiro-Filho *et al*., 2002). Despite the proven efficacy of stand-alone morphometric techniques obtained in higher-level taxonomic investigations, complementary genetic data are essential to gain greater insight into variation within populations (Sudarto *et al*., 2010).

1.2 Current techniques used to obtain morphometric data on cetaceans

Traditionally, three main avenues exist for the collection of morphometric data on cetaceans: 1) the use of post-mortem specimens; 2) live captive subjects; and 3) capture-release health programs (Clark & Odell, 1999; Murphy & Rogan, 2006; Wells *et al.,* 2009). For some dolphin populations, post-mortem examinations remain the only avenue available to gather information on morphological and functional characteristics, because of ethical and accessibility constraints associated with live-animal sampling (Neuenhagen *et al.,* 2007). The opportunity to conduct these examinations may arise from stranding events (Murphy & Rogan, 2006; Fortune *et al.,* 2012; Chivers *et al*., 2016), as well as incidental (Frainer *et al*., 2015) and deliberate capture (Hoekstra *et al*., 2002). Despite the increased measurement accuracy associated with physical examinations, the utilisation of post-mortem examinations in research is limited by their random occurrence. The greatest challenge researchers face with respect to post-mortem research is developing sufficiently representative sample sizes over a short period of time (Evans *et al.,* 2003; Fortune *et al.,* 2012). In addition, the haphazard nature of stranding events may contribute to the over or under-representation of groups or samples, due to a lack of sampling structure (Epperly *et al*., 1996; Siebert *et al*., 2006). For example, it is possible that dietary constraints, post-mortem morphological changes, or pathology affect the representativeness of deceased animals, thus tainting the validity of research findings (Peltier *et al*., 2012). Despite their limitations, post-mortem events will continue to provide valuable morphometric data; however, it is imperative that researchers delineate the suitability and statistical validity of their post-mortem derived inferences.

Captive settings facilitate unhindered access to live subjects without the need for rushed assessments, and data collection processes are usually of high quality and repeatable. A similar level of consistent access to the same live subjects would be difficult to achieve with free-ranging cetaceans, as several species demonstrate highly-dynamic, short- and long-term movement patterns (Sprogis *et al*., 2016). However, as in the case of post-mortem subjects, the representativeness of captivity-derived morphometric data has been subject to debate due to potentially differentiating factors relating to environment, diet and energy expenditure (Cheal & Gales, 1991; Kastelein *et al*., 2016). Several studies reported identical growth parameters between captive and free-ranging delphinids (Ridgway & Fenner, 1982; Cheal & Gales, 1991; Clark & Odell, 1999; Robeck *et al*., 2015), while others described the opposite, with contrasting postnatal growth rates and age-to-weight ratios (Cheal & Gales, 1991) as well as dorsal fin morphology (Kastelein *et al*., 2016).

An alternative to using captive animals entails the sampling of individuals in free-ranging populations through capture-release programs. These programs employ temporary capture techniques to sample free-ranging specimens before they are again released. For example, the Bottlenose Dolphin Health and Risk Assessment project (Fair *et al*., 2006; Wells *et al*., 2009) enables biologists to measure known individuals with some degree of sampling structure and measurement accuracy, with the additional possibility of measuring resident specimens repeatedly over time. Given the highly invasive use of capture-release programs, the use of alternative data collection techniques is necessary.

Recent technological advances initiated the use of indirect sampling for some cetacean species. Indirect sampling does not rely on the capture of animal subjects because samples are obtained at distance by using equipment such as unmanned aerial vehicles (UAVs) carrying cameras (Christiansen *et al*., 2016), laser pointers (Durban & Parsons, 2006; Rowe & Dawson, 2008) and range finders (Jaquet, 2006). While these techniques are relatively new

within the established field of cetacean morphometrics, multiple studies investigated dorsal fin characteristics (Brown *et al*., 2016), total length (Growcott *et al*., 2011) and growth rates (Best & Ruther, 1992) using pixel quantification and photogrammetry. Most life history traits (e.g. age at sexual maturity, age at weaning) are age-specific, and thus the importance of understanding population-specific age structure is essential.

1.3 The importance of age-specific demographic data in wildlife biology

Population studies (such as population viability analyses) rely heavily on demographic parameters to assess the vulnerability of a population or species, as well as their recovery potential, both with and without management intervention (Zambrano *et al*., 2007). Age-structured matrices (such as the Leslie Matrix) allow researchers to describe the growth and age distribution of a closed population (Caswell, 2012), by highlighting possible differences in vital rates among extant individuals across a range of classes, such as age groups, life stages or size (Caswell, 2012). Vital rates are class-specific rates pertaining to survival, fecundity and individual growth (Morris *et al*., 1999) and are used as metrics for defining the viability of a population and for allowing for the implementation of management actions that target specifically the rates of concern (Morris *et al.,* 1999). As an example, in Western Australia, Manlik *et al*. (2016) documented that Bunbury's declining bottlenose dolphin (*Tursiops aduncus*) population yielded a lower reproductive rate than the more-stable Shark Bay population, suggesting that the difference in viability between these populations is due to contrasting birth rates. Therefore, increasing the reproductive rates of the Bunbury population should be the main management priority, as this would be the most effective tool for reversing the population decline. Vital rates in age- or stage-structured models are heavily reliant on population-specific demographic data, as it describes the rates of transition from one stage to the next that are used to model population viability (Morris *et al*., 1999). However, the collection of such demographic data can be troublesome, with few age estimation methods available.

1.4 Current age estimation techniques of free-ranging marine vertebrates

The age of an organism can be estimated through a variety of techniques; However, traditionally, there has been a dependence on either invasive means of data collection or the use of dead specimens (Campana, 2001). Current age estimation methods are usually assigned to three broad classes: molecular analyses (George *et al*., 1999), long-term monitoring of individuals (Krzyszczyk & Mann, 2012) and the quantification of growth layer groups within a calcareous structure (Campana, 2001). Molecular analyses rely on intrinsic changes occurring chronologically between chemical compounds, resulting in a quantifiable ratio that correlates with dentinal age (Garde *et al*., 2010; Polanowski *et al*., 2014). Long-term photo-identification allows researchers to monitor individuals over time (Wursig & Wursig, 1977; Krzyszczyk & Mann, 2012), where long-term birthing histories can be developed for mature females. The majority of age estimations are derived from growth increments within internal and external structures that relate to a temporal period. The latter has been applied across a range of invertebrates including bivalve shells (Vadopalas, 2011), cephalopod statoliths (Natsukari & Komine, 1992) and cricket exoskeletons (Zuk, 1987), as well as vertebrate groups such as fish (Pannella, 1971) and mammals (Dellabianca *et al*., 2012). The following section focuses primarily on the current age estimation techniques of free-ranging cetaceans.

In toothed whales (i.e. odontocetes), dentinal growth layer groups (GLGs) are subsequently deposited following the neonatal line, which is a hypo-calcified layer formed at the time of birth (Lockyer *et al*., 2007). This allows for the quantification of annually secreted crystallised or opaque zones found within dentinal tissue, providing researchers with an age estimate in the same way as otoliths of fish (Campana, 2001). For baleen whales (i.e. mysticetes), GLG formations in ear plugs have been used to determine age estimates, however the temporal resolution of these GLG increments are inconsistent and species-dependent. For example, Lockyer (1984) provided evidence supporting an annual formation of GLGs in fin whale

(*Balaenoptera physalus*), minke whale (*Balaenoptera acutorostrata*) and pygmy blue whale ear plugs (*Balaenoptera musculus brevicauda*), while both annual and biannual GLG formations have been documented in humpback whales (*Megaptera novaeangliae*; Clapham, 1992; Gabriele *et al*., 2010). Though baleen plate thickness has been applied as an age estimation metric, the isotopic signatures contained within the keratinous baleen plates have also proven valuable for the assessment of seasonal foraging dynamics (Lubetkin, 2008) as well as life history parameters relating to the onset of reproductive maturity (Hunt *et al*., 2014).

Aspartic acid racemisation is the most predominant of molecular analyses and aims to measure the degree of amino acid racemisation (i.e. the conversion of an active compound into a racemic compound) within a metabolically stable protein of an individual (George *et al*., 1999; Lubetkin, 2008). In neonatal specimens, the ratio between D-amino and L-amino carbohydrates is approximately zero, and thus the extent to which the racemisation process has progressed within an animal can be used to infer age at the time of death (George *et al*., 1999; Garde *et al*., 2012; Nielsen *et al*., 2013; Pleskach, 2016). Although this technique has proven successful, with a relatively low error rate and a high level of precision, the wider application of this technique is still hindered by its reliance on deceased specimens. Recently, Polanowski *et al*. (2014) introduced a technique utilising age-associated DNA methylation. This method enables age estimates to be obtained from live animals, by means of non-lethal biopsy sampling. However, to unlock its considerable potential, this research approach needs to be developed further.

It is possible to identify individual cetaceans using natural markings visible on the dorsal fin, body surface or tail flukes (Wursig & Wursig, 1977; Payne *et al*., 1983). Long-term, photo-identification programs allow researchers to follow individuals over time, providing a reliable account of age and individual history. These data are essential to investigating life-history

traits and population demographics (Manlik *et al*., 2016; Smith *et al*., 2016), foraging ecology (Ford *et al*., 2010; Kopps *et al*., 2014), spatial and temporal distribution (Irvine *et al*., 1981; Sprogis *et al*., 2016) and social behaviour (Connor & Krutzen, 2015). However, the intensity of sampling effort within these programs influences the level of error associated with the age estimates. For example, the amount of time elapsed between sightings will determine how accurate age estimations are, with more frequent at-sea sampling effort generally providing greater chances of locating and documenting the animals more often.

1.5 Combining morphometric and age-specific data to manage populations

Improving our knowledge of demographic and morphological processes can contribute valuable insights into the life history strategies of species, as well as the potentially-unique characteristics of inter-specific populations. In addition, understanding the manner in which these ecological, morphological and demographic processes interact with one another is vital when seeking solutions to conservation issues (Blomquist *et al*., 2009). When a population is subjected to unsustainable exploitation or environmental pressures, growth and age-specific parameters (such as length-at-sexual-maturity) are known to change as a compensatory mechanism (Fearnbach *et al*., 2011). If such changes are detected, managers can focus their mitigative efforts more effectively. For example, fisheries scientists must understand the population dynamics of separate fish stocks in order to determine appropriate sustainable yields. This involves evaluating the ability of individual fish reaching a predetermined size or reproductive stage (i.e. recruitment), total mortality comprising of both natural and harvest-associated mortality, as well as estimating population biomass using the rates at which individual fish increase in length and weight (Hart *et al*., 2013).

For cetaceans, researchers compare life history strategies between inter- and intra-specific populations and management units, in which age-specific patterns play a central role in viability analyses describing how individuals allocate resources to important traits, such as

growth, reproduction and survival (Enberg *et al*., 2008). Demographic and morphological data can be consolidated using mathematical growth functions, allowing researchers to describe, compare and predict the longitudinal growth and development patterns of populations (McFee *et al*., 2010). These growth models are also applied as a means of comparing the growth parameters of vertebrate populations, including but not limited to maximum (asymptotic) length, length at birth or first reproduction, as well as girth and mass (Read *et al*., 1993). Such comparisons are vital for delineating stocks that possess independent life history strategies, thereby justifying the need for specialised conservation management approaches (Cunha *et al*., 2014).

1.6 Development of photogrammetric techniques within morphometric studies

Traditional morphometric techniques (such as the use of physical measurements) have made it possible for biologists to acquire accurate morphological data on free-ranging vertebrates. However, there are inherent weaknesses associated with this approach, relating specifically to sample size and limited non-invasive data collection methods. The term 'photogrammetry' is the quantification or measurement of a subject using photographic techniques (Best & Rüther, 1992). Currently, three forms of photogrammetry have been developed: stereo, aerial and remote laser photogrammetry.

In stereo photogrammetry, two cameras are used in parallel orientation to take a composite image of an object simultaneously (**Figure 1.1**). The distance between the two cameras as well as their lens magnifications are known, allowing for the dimensions of a subject to be quantified based on its horizontal displacement within the pair of photographs (Klimley & Brown, 1983). This technique has proven useful in obtaining body length and fine-scale

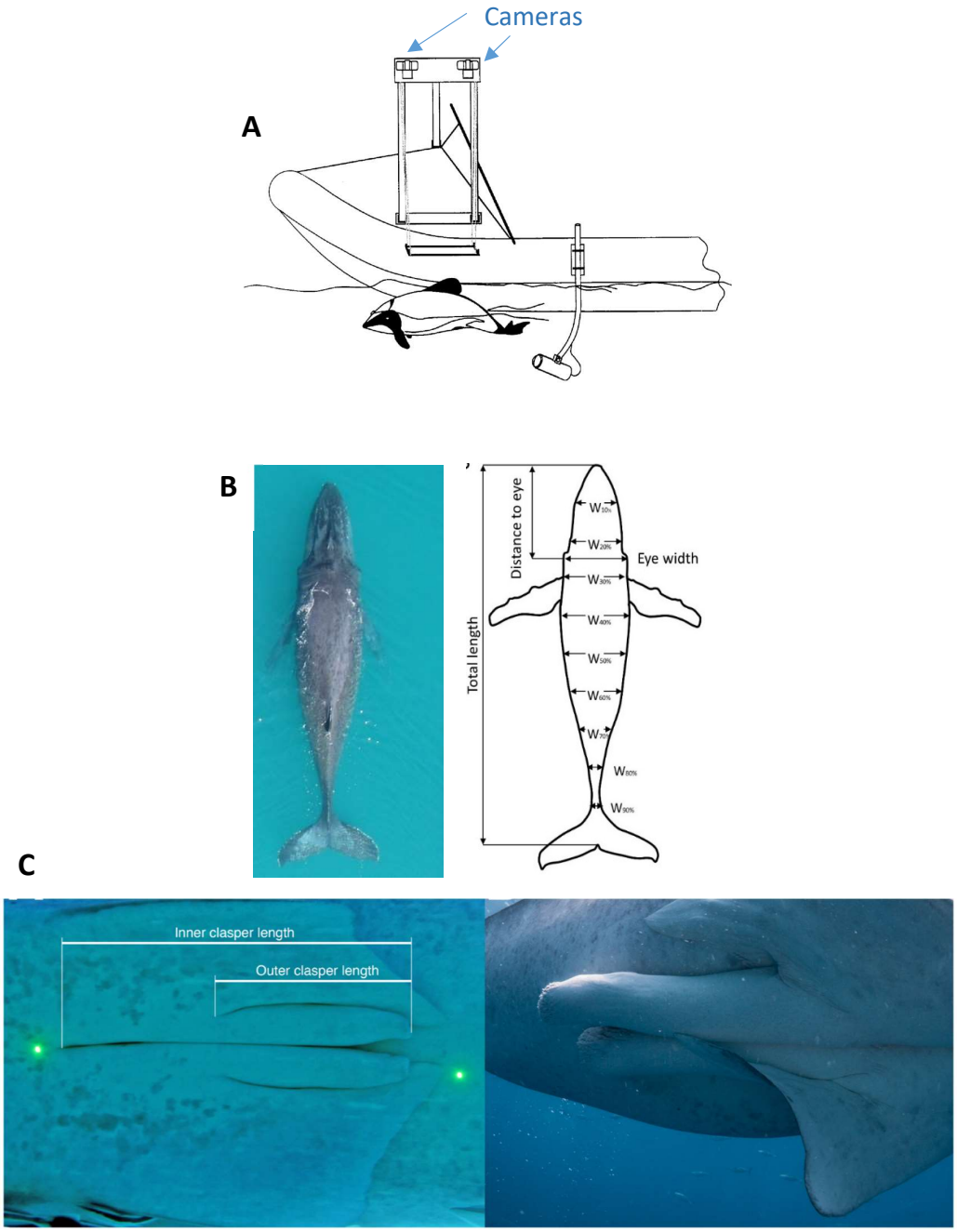

Figure 1.1 Examples of the data collection techniques associated with each of the three photogrammetry techniques: **A**) stereo-photogrammetry set-up used to obtain measurements of Hector's dolphins (*Cephalorhynchus hectori*; Brager *et al*., 1999); **B)** aerial—photogrammetry of a humpback whale (*Megaptera novaeangliae*) obtained from an unmanned aerial vehicle (UAV), including a diagram overviewing locations of where body-width was measured (Christiansen *et al*., 2016); **C)** remote laser photogrammetry measuring clasper length to infer sexual maturity of male whale sharks (*Rhincodon typus*; Rohner *et al*., 2015).

Table 1.1 A summary table listing each of the three photogrammetry techniques and their respective measurement targets, such as total body length (TBL). Studies with example species showcase the morphometric index used to substitute TBL, as well as the data collection platform, example species, respective sample sizes and level of precision error achieved using each technique. Blowhole-to-dorsal fin length is abbreviated as BH-DF.

Photogrammetry Technique	Measurement Target	Morphometric Index used	Data Collection Platform	Example Species	Sample Size	Precision CV %	Reference
Stereo	TBL	BH-DF	Research Vessel	Hector's dolphin *Cephalorhynchus hectori*	35	-	Brager *et al*., (1999)
	TBL, Position of individuals	-	Underwater	Scalloped hammerhead shark *Sphyrna lewini*	122	5.00	Klimley & Brown (1983)
	TBL	BH-DF	Research vessel	Sperm whale *Physeter macrocephalus*	41	4.38	Dawson *et al*. (1995)
	TBL	-	Helicopter	Killer whale *Orcinus spp*	220	1.90	Pitman *et al*. (2007)
Aerial	TBL	-	Fixed-wing aircraft	Gray whale *Eschrichtius robustus*	214	4.20	Sumich & Show (2011)
	TBL	-	Helicopter	Southern right whale *Eubalaena australis*	144	4.56	Best & Ruther (1992)
	TBL, body width, distance to eye,	-	UAV-drone	Humpback whales *Megaptera novaeangliae*	134	-	Christiansen *et al*. (2016)
	Multiple	-	Captive	Western gorilla *Gorilla gorilla*	4	0.01	Galbany *et al*. (2016)
Remote laser	TBL, body mass	-	Terrestrial	Galapagos sea lion *Zalophus wollebaeki*	87	2.90	Meise *et al*. (2014)
	Clasper length	-	Underwater	Whale shark *Rhincodon typus*	168	0.17	Rohner *et al*. (2015)
	Horn dimensions	-	Terrestrial	Alpine ibex *Capra ibex*	7	3.14	Bergeron (2007)
	Dorsal fin dimensions	-	Research vessel	Hectors dolphin *Cephalorhynchus hectori*	34	3.71	Webster *et al*. (2010)
	Disk length and width	-	Underwater	Manta ray *Manta alfredi*	274	1.46	Deakos (2012)
	TBL, Head width	-	Underwater	Great hammerhead shark *Sphyrna mokarran*	16	-	O'Connell & Leurs (2016)
	TBL, shoulder height	-	Terrestrial	Asian elephant *Elephas maximus*	1	6.00	Wijeyamohan *et al*. (2012)

spatial movement data of several free-ranging marine vertebrates (Klimley & Brown, 1983; Dawson *et al*., 1995; van Rooij & Videler, 1996; Brager *et al*., 1999; see **Table 1.1**).

However, the cumbersome nature of the hardware required for stereo photogrammetry severely limits its practicality *in-situ*. For example, Brager *et al*. (1999) used a 0.6 X 0.8 m metal frame to secure two cameras onto the front of their 4.5 m research vessel (**Figure 1.1**), and found the system to be immobile and restrictive, requiring calm sea conditions and approachable dolphin subjects.

In aerial photogrammetry, images are collected via manned aerial vehicles such as helicopters, fixed-wing aircrafts, and more recently, via unmanned aerial vehicles (UAV) such as drones. The measurement scale in each photograph can be calculated by dividing the distance between the camera and subject (i.e. altitude) by the focal length of the camera lens (Pitman *et al*., 2007; Mocklin *et al*., 2010). In addition, it is also possible to convert pixel counts into accurate length measurements, as demonstrated by Christiansen *et al*., (2016), who used the length of their research vessel as a scale reference within photographs (**Figure 1.1**; **Table 1.1**). Recent technological advances have increased access to remotely operated UAVs, enabling researchers to obtain valuable morphometric data in a less invasive and cost-effective manner compared to traditional aircraft.

In recent decades, remote laser photogrammetry gained popularity due to its simplicity and mobility (Durban & Parsons, 2006; Rowe & Dawson, 2008). The system comprises two laser pointers mounted in parallel orientation and projecting two laser dots onto the surface of a study subject (Bester & Bruyn, 2015; Rohner *et al*., 2015; **Figure 1.1**). Because the distance between the two laser points is known, the corresponding pixel count can be converted into an absolute measurement (Bergeron, 2007). The lightweight laser system can be mounted on a camera lens, allowing for laser-derived measurements and photo-identification data to be obtained simultaneously (Webster *et al*., 2010). The minimal logistical requirements and

cost effectiveness of remote laser photogrammetry are considered significant advantages in addition to its high level of measurement accuracy and precision. The simple yet effective nature of remote laser photogrammetry has resulted in a diverse range of applications within wildlife biology, including both terrestrial and marine mammals as well as large, mobile elasmobranch species (see **Table 1.1** for examples). While remote laser photogrammetry is not a novel morphometric technique, its use with small cetaceans has been limited to a handful of studies (Rowe & Dawson, 2008; Webster *et al*., 2010; Cheney *et al*., 2015).

1.7 Thesis objectives

Future applications of these data appear promising, not only in relation to the intrinsic value of morphometric data but also with respect to the way these data are collected. However, as is the case for many morphometric techniques, measurement error can significantly affect the quality of the data obtained. Despite this, the level of precision achieved with remote laser photogrammetry remains acceptable as demonstrated by **Table 1.1**. The accuracy of this technique depends on several sources of error present in the field. While these potential sources of error have been subjected to preliminary examinations within several studies (Rowe & Dawson, 2008; Webster *et al*., 2010), no comprehensive analyses are available. Accordingly, it is essential to continue developing the knowledge of how underlying processes affect the precision and accuracy of remote laser photogrammetry. This can be achieved by a means of technique development and the quantification of error. Hence, the **primary objective** of the current study is to:

1. **Investigate the feasibility and precision of remote laser photogrammetry, as a means of obtaining morphometric data on free-ranging coastal bottlenose dolphins.**

   The secondary objectives of the study will demonstrate the value of remote laser photogrammetry by providing empirical examples of the uses of this non-invasive technique, including:

1. **Developing length-at-age growth curves using dolphin populations of known-age.**

   Longitudinal demographic data will be combined with laser-derived length data to fit population growth curves. By fitting growth models to age-to-length data, valuable insights can be gained into the growth and life history processes of coastal bottlenose dolphins residing in Bunbury, Mandurah and Shark Bay, Western Australia.

2. **Comparing morphological differences between geographically-separated populations.**

   The use of asymptotic growth curves facilitates growth comparisons between geographically-separated populations. In addition, this data would provide the basis for future studies that investigate the biological, ecological and genetic factors influencing intra-specific variations in growth.

2. Methods and Materials

The accuracy and precision of laser-derived measurements was investigated and quantified using a range of experiments (**Table 2.1**). Once ground-truthing of the technique was complete, laser photogrammetry was implemented to obtain length data on these populations of Indo-Pacific bottlenose dolphins.

2.1 Laser photogrammetry system

2.1.1 System setup

To measure the blow hole (BH) to dorsal fin (DF) length of free-ranging dolphins, a paired laser system was used and comprised of a 12.3 MP Nikon D300s camera body coupled with a Nikon 80-400mm f/4.5-5.6D ED telephoto lens. A custom-made mounting block contained two aluminium laser modules and was attached to the lens using a factory-made tripod mount, forming a compact, mobile system (**Figure 2.1A**). The laser system was operated via a finger-touch on/off switch, with synchronisation between the camera shutter and laser modules facilitated by a cable connected to the ten-pin port on the camera body. The commercially available green laser pointers (BEAMSHOT GreenBeam 1000, wavelength 532 nm) provided superior daylight performance compared to red lasers. The output power of the lasers was 5mW (Class IIIa) and did not pose any significant health risk to the dolphins or researchers, because the exposure was limited by safe-use protocols. These protocols involved directing the laser dots posterior to the dolphin's head and positioning all researchers behind the photographer.

2.1.2 Laser calibration procedure

Prior to use each field day, the orientation of the laser projections was tested using a calibration board placed at eye-level and perpendicular to the camera (**Figure 2.1B**). During the calibration procedure, the laser camera was mounted on a tripod and levelled, thereby ensuring that the camera was positioned on the same horizontal plane as the calibration

board. The calibration board contained two parallel vertical lines 10 cm apart, that served as reference points for the two laser projections (see **Figure 2.1B**). If the lasers failed to align with the two reference points, adjustments were made by rotating the vertical and horizontal-configured grub screws on the laser modules until they were aligned.

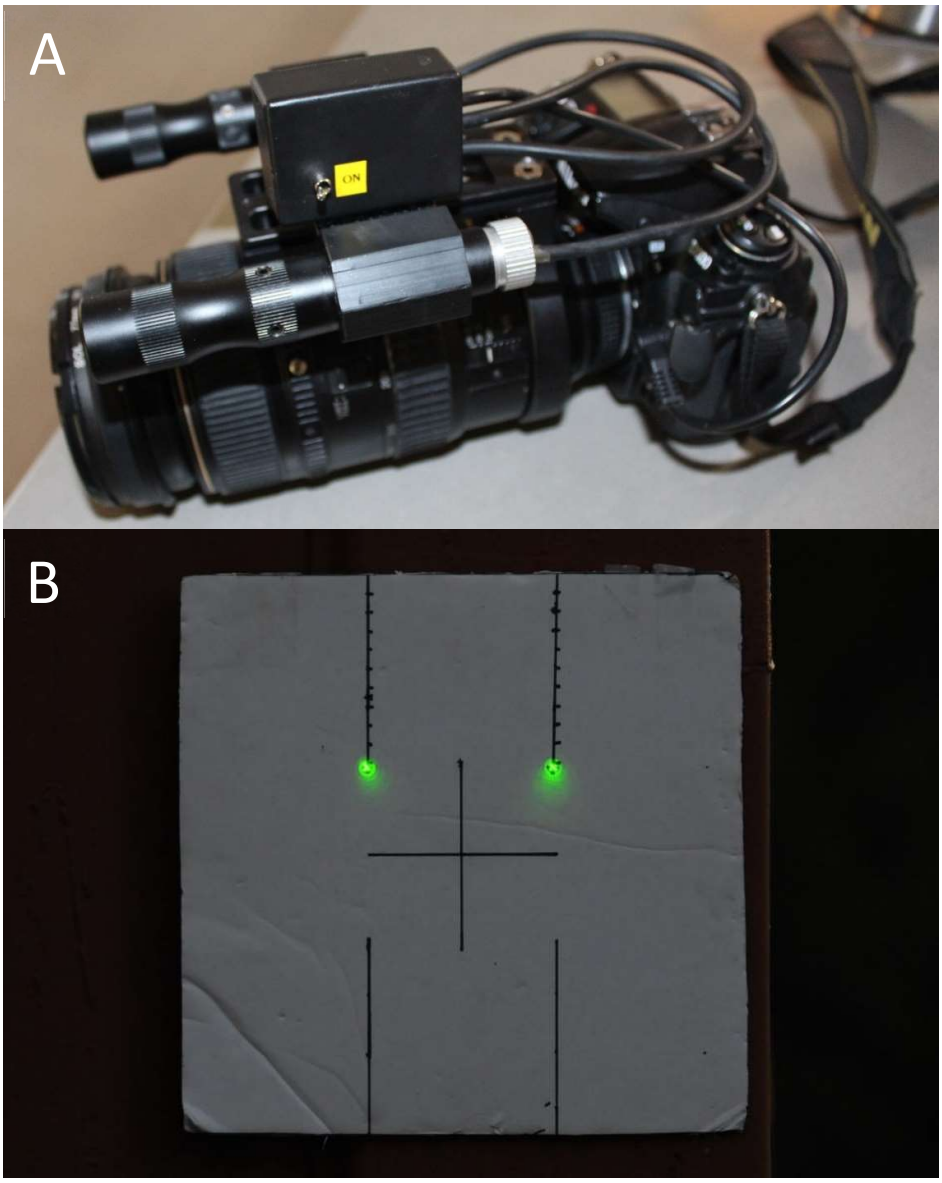

Figure 2.1 A) Camera with the mounted laser system; and **B**) the calibration board used to calibrate the paired lasers. The distance between the two green dots projected by the lasers onto the calibration board is ten centimetres.

The grub screws were tightened once the laser projections were positioned 10 cm apart and parallel. Photographs were then taken in five-metre distance increments, ranging from 5 m to 20 m, and ensuring that the laser projections were consistent with the reference points across the distance spectrum.

Following each boat survey, the relative position of the laser dots was tested and recorded by photographing the calibration board throughout the 5 to 20 m distance spectrum. It was then possible to measure and compare the laser calibration prior to, and following, a boat survey. In poor weather conditions, or in the event of an unexpected impact causing the position of the lasers to change, the lasers were recalibrated *in-situ* by using the calibration board at a closer distance of approximately 4.5 m. If this was not possible, the boat survey was aborted and the data discarded.

2.2 Potential sources of measurement error

Measurement data obtained through remote laser photogrammetry are susceptible to several sources of error that have the potential to adversely affect the accuracy and precision of measurements (Durban & Parsons, 2006; Leurs *et al*., 2015). Measurement *accuracy* can be defined as the extent of cohesion between known and remotely-measured values, where known values correspond to the true measurement of a subject. The discrepancy between the two values can be influenced by systematic errors stemming from laser and camera equipment as well as calibration, image selection and measurement procedures (Galbany *et al*., 2016).

Measurement *precision*, on the other hand, can be defined as the level of agreement between observed measurements of the same subject, obtained in conditions deemed to be equivalent (Galbany *et al*., 2016). This can also be influenced by systematic errors in the form of measurement procedures. For example, multiple observers may produce differing measurements of the same animal, because of poorly defined measurement protocols.

To counter this, throughout the current study, standardised protocols were developed for both image selection and measurement processes and were carried out by the same individual. To develop these protocols, however, it was important to identify the sources of error present and the extent to which these sources influence both measurement accuracy and precision.

2.2.1 Measurement error associated with horizontal angle and distance to dolphin

When measuring free-ranging dolphins using laser photogrammetry, the most influential source of error is horizontal angle error, which occurs when the photographer and surfacing dolphin are not oriented perpendicular to each other along the horizontal plane (Durban & Parsons, 2006; Rowe & Dawson, 2008; Webster *et al*., 2010).

Table 2.1 Summary table describing the various experimental objectives and designs used to determine the feasibility of laser photogrammetry.

	Potential sources of error			Measurement accuracy
EXPERIMENTAL DESIGN	horizontal angle	horizontal distance	body curvature	compare physical and laser measurements
Two-dimensional calibration board	Y	Y	N	N
Three-dimensional dolphin replica model	Y	Y	Y	N
Post-mortem dolphin subjects	Y	Y	Y	Y

I quantified measurement errors associated with horizontal angles and distances using two experiments: the first utilised a two-dimensional calibration board, while the second experiment was conducted using a three-dimensional dolphin replica model (**Table 2.1**).

2.2.2 Error experiment using a two-dimensional calibration board

To quantify the measurement errors associated with the horizontal angle and the distance between the camera and dolphin, an experiment was conducted using the two-dimensional calibration board previously described (**Figure 2.1B**). The two outlines marked on the board represented a known, 10-cm distance, and are used as a scale reference for measurements. With the board secured on a tripod at eye-level, a measuring tape was placed perpendicular to the tripod and, to a distance of 25 m.

The board was placed at incremental horizontal angles ranging from perpendicular (hereby referred to as 0°) to 75° from perpendicular to the camera. The board was rotated and photographed in five increments. This process was repeated at 5, 10, 15, 20 and 25 m distances. At each stage, ten high resolution photographs were taken with the two laser pointers positioned on the board by the photographer.

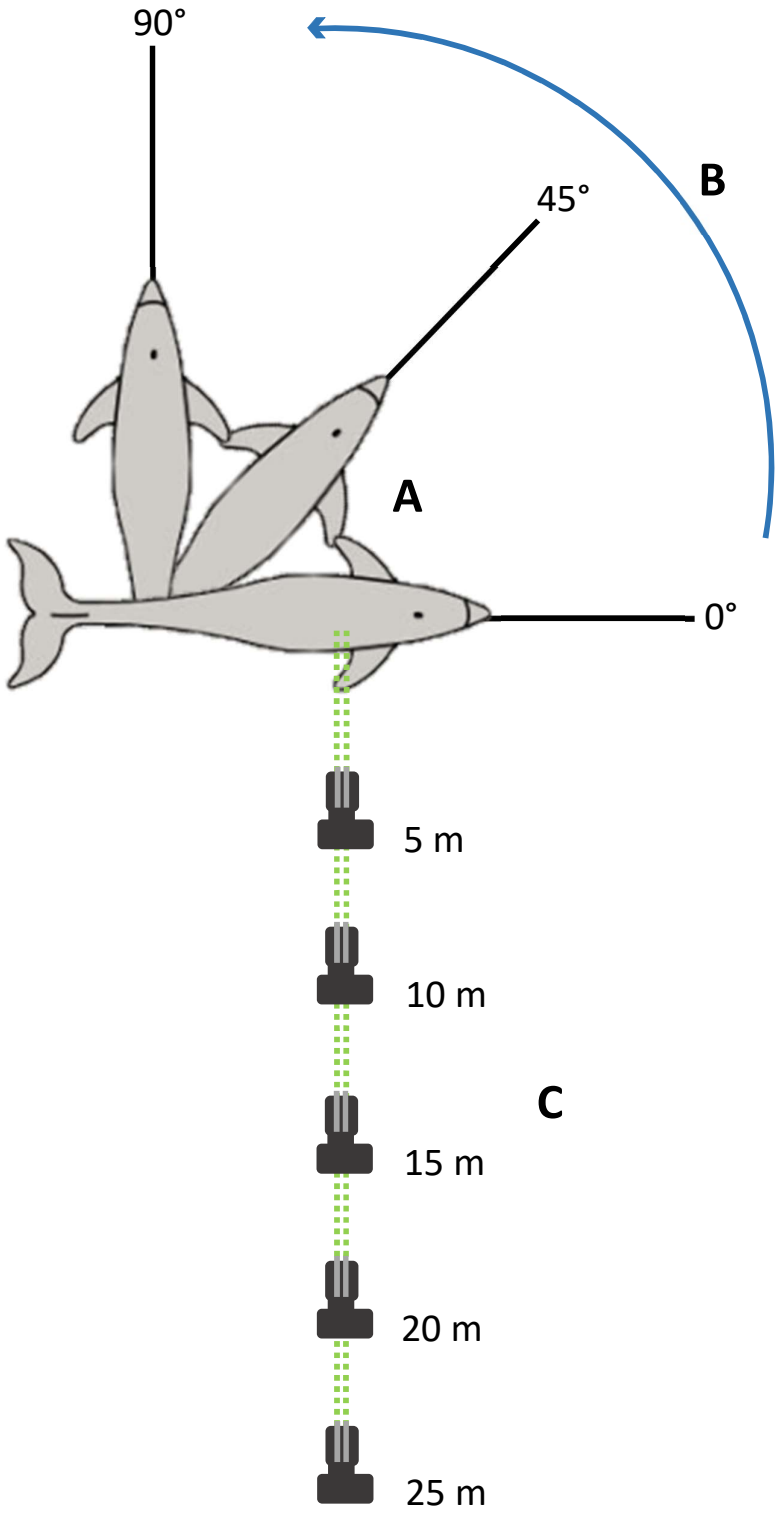

Figure 2.2 Schematic description of the three-dimensional error experiment used to test angle, distance and body curvature. **A** & **B** represent the dolphin being rotated in 15° increments, while **C**) shows the five (5-25m) distance increments. This process is identical for the two-dimensional error experiment. Dolphin schematic by D. Weihs.

2.2.3 Error experiment using a three-dimensional dolphin replica model

I also quantified potential errors associated with horizontal angles and distances between the laser camera and study subjects on a three-dimensional surface. Specifically, I used a replica dolphin model to simulate the convex shape of a dolphin's lateral surface, as it was unknown whether this could cause differing error estimates compared to the flat surface. Previous studies attempted to quantify the error associated with both horizontal angle and distance (Webster *et al*., 2010; Leurs *et al*., 2015); however, to date, no experiments investigated the possible influence of body curvature on error measurements. In the current experiment, the lateral surface of the dolphin replica (see **Figure 2.3**) was separated into three dedicated zones: upper or dorsolateral (**A**); mid or lateral (**B**); and lower or ventrolateral (**C**).

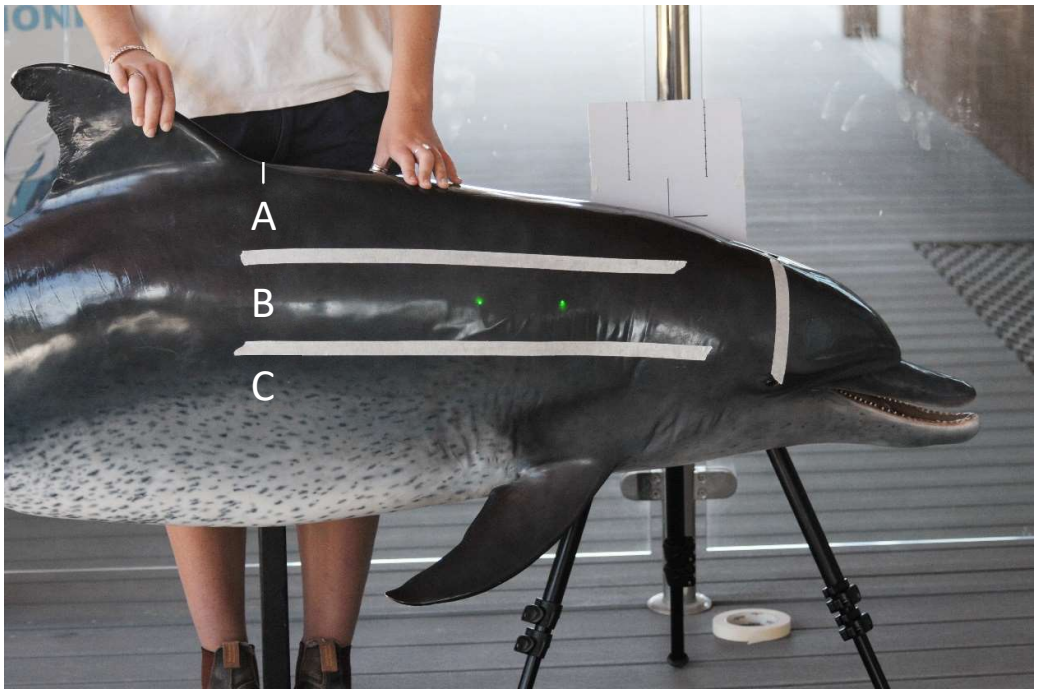

Figure 2.3 Example photograph of the three-dimensional replica model exhibiting the three body curvature zones: upper zone (**A**); mid zone (**B**); and lower zone (**C**).

Although the experimental procedure was similar to the calibration board experiment, there were some differences worth mentioning. The laser dots were positioned inside each of the curvature zones, with five to ten high-resolution images taken at each zone, distance and angle increment. The distances tested were identical to those used in the previous experiment, i.e. 5m to 25m in 5m increments. However, it was difficult to rotate the dolphin replica in five degree increments with any degree of confidence. As a result, rotational increments of approximately 15° were employed in order to gain an acceptable level of confidence in the accuracy of our angle.

2.2.4 Error experiment using opportunistic post-mortem subjects

Post-mortem events of freshly-stranded or by-caught dolphins provided opportunities to investigate measurement errors further and allowed for comparisons between laser photogrammetry measurements with manual morphometric measurements using a measuring tape (**Figure 2.4**).

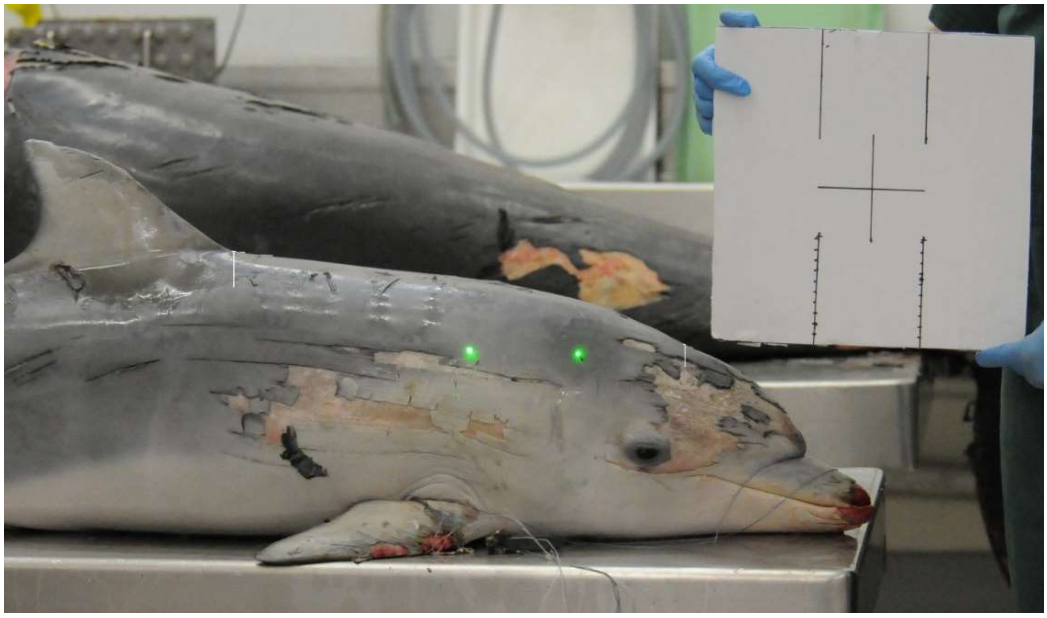

Figure 2.4 Example photograph of the two green laser dots projected onto a post-mortem dolphin subject**,** to compare differences between manually- and laser-derived measurements.

In addition, a flexible measuring tape was used to record the blowhole-to-dorsal fin (BH-DF) length of each dolphin. Since all free-ranging dolphins were measured using the straight distance between the blowhole and anterior origin of dorsal fin, all post-mortem subjects were measured in an identical manner, as later described in section **2.4.5**.

To test for significant differences in laser-derived measurements in response to horizontal angle, distance and body curvature, a three-way analysis of variance (ANOVA) was conducted using laser-derived measurements as the dependent variable. To determine whether any of the potential error sources influenced one another, interaction effects were added to the ANOVA procedures.

A paired t-test was carried out to test whether any significant differences were present between the laser-derived and physical measurements of post-mortem subjects. All statistical tests performed in the current study were carried out using R version 3.2.4 (R Core Team, 2013).

2.3 The relationship between blowhole-to-dorsal fin and total body length

Opportunistic post-mortem subjects were also used to investigate the relationship between BH-DF length and total body length (TBL). Since long-term increases in BH-DF length and TBL were consistent (allometric), this relationship would be best described using linear terms (Clark & Odell, 1999). Therefore, to test whether this relationship was true in *T. aduncus*, linear regression was employed using manual BH-DF and TBL measurements obtained during necropsy examinations.

2.4 Applications of remote laser photogrammetry

2.4.1 Study sites

Laser-derived measurement data on Indo-Pacific bottlenose dolphins (*Tursiops aduncus*) were obtained from three study locations (**Figure 2.5**): Shark Bay and Bunbury, Western Australia (WA) provided opportunities to utilise known-age animals within previously studied populations; while Mandurah, WA, offered access to unknown-age, bottlenose dolphins within a study population.

The bottlenose dolphin population inhabiting the coastal waters off Bunbury (33°32' S, 115°63' E) served as the primary focus of the study (**Figure 2.5C**). Initial attempts at low-effort monitoring of Bunbury's dolphin population first commenced in 1989 (**Table 2.2**), with the establishment of the Bunbury Dolphin Trust (Dolphin Discovery Centre, pers. comm). In 2007, the South West Marine Research Program (SWMRP) was launched with the aim of assessing the long-term viability of the *T. aduncus* population. Through the longitudinal research conducted by the SWMRP, the Murdoch University Cetacean Research Unit (MUCRU) has been able to identify and catalogue over 500 individuals through boat-based photo identification transect surveys.

Laser photogrammetry data were also collected in Shark Bay, WA, located approximately 1,000 km north of Bunbury. For the purposes of the current study, sampling was conducted heading out of Monkey Mia (25°47' S, 113°43' E), in the eastern gulf (**Figure 2.5A)**. The Shark Bay Dolphin Project (SBDP) has been studying a population of over 1,600 recognized individuals since 1984, making it the second-longest-running dolphin research project worldwide (Karniski *et al*., 2015; **Table 2.2**). Monkey Mia is also the site of a long-term provisioning program, where qualified rangers provision carefully-selected individuals during beach visitations that take place on a near-daily basis.

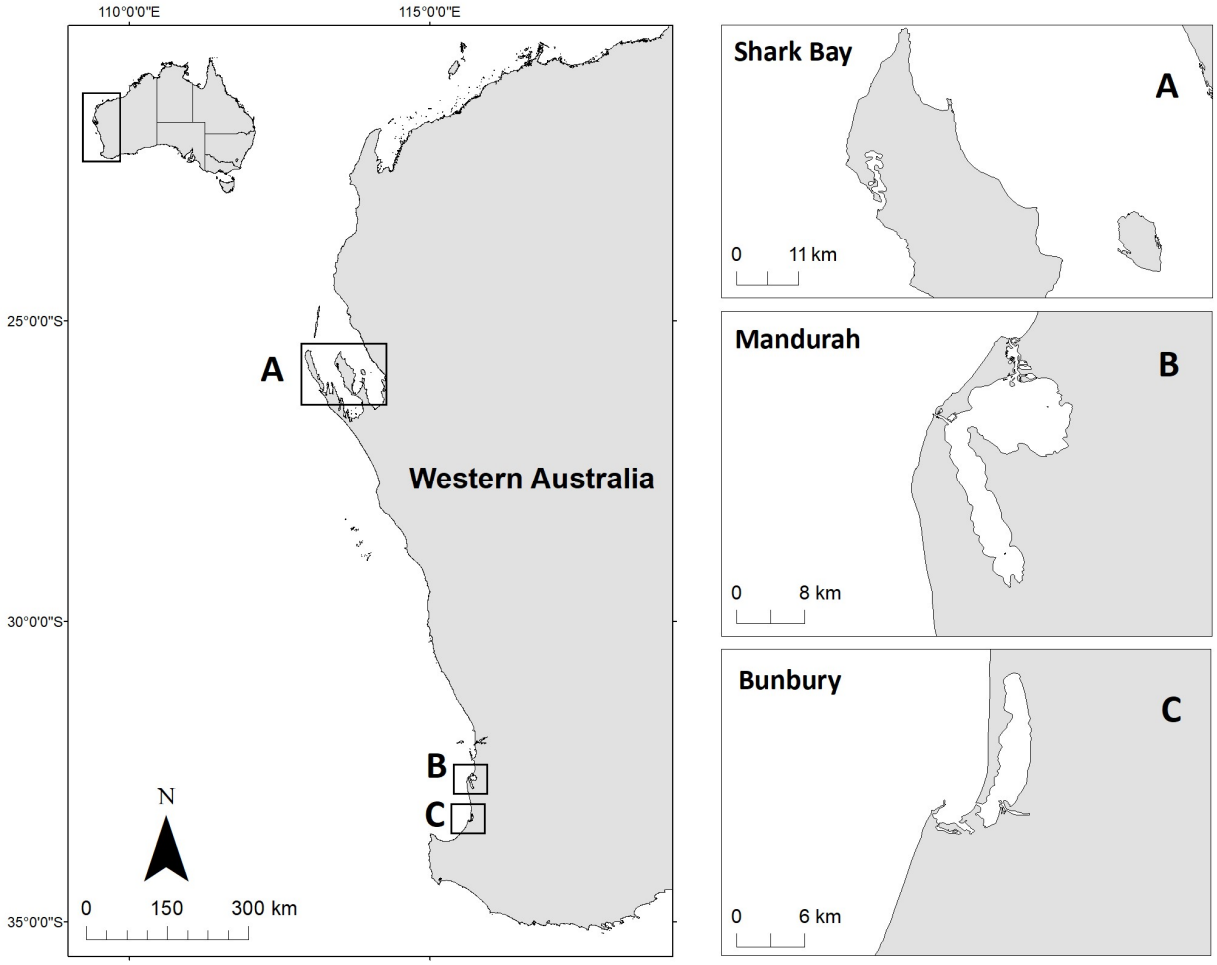

Figure 2.5 A map of the Western Australian coast, with the relative positions of each of the study sites noted. Enlarged inset maps of each of the Shark Bay (**A**), Mandurah (**B**), and Bunbury (**C**) study sites are exhibited on the right.

Ad-hoc food provisioning occurred in Monkey Mia since 1964 (**Table 2.2**), with some limited collection of demographic data recorded prior to the commencement of official monitoring in the 1980s. The accessibility and reliability of these dolphin visits, coupled with the shallow, calm conditions provide an excellent platform from which to collect a variety of data on free-ranging coastal dolphins. The population of *T. aduncus* residing in Mandurah, WA, (32°32' S, 115°44' E; **Figure 2.5B**) were sampled as part of the 'unknown age' population (**Table 2.2**).

Table 2.2 A summary of the research projects, their commencing years and their respective population size estimates. The time period of data collection is also provided.

Site	Commencement of dedicated dolphin research (year)	*Ad-hoc* data available from (approx. year)	Estimated population size	Laser-derived data collection period
Bunbury	2007	1989	500[1]	May 2016 – January 2017
Shark Bay	1984	1960s	1,600[2]	October 2016
Mandurah	2016	1991	400[3]	June 2016 – March 2017

[1] Symons (August, 2016, pers. comm)
[2] Karniski *et al*. (2015)
[3] K. Nicholson (March, 2017, pers. comm)

Mandurah is located approximately 100 km north of Bunbury, and exhibits an identical Mediterranean climate. Since commencement in January 2016, the Mandurah Dolphin Research Project (MDRP) has identified approximately 400 individual dolphins within the 520 km^2 study area (K. Nicholson, *pers. comm*). However, because the research effort has been short-term, demographic data for reliable individual dolphin age estimates are limited. Long-term citizen science efforts and stranding records made it possible to establish reliable age estimates for approximately 28 individuals residing in the Peel-Harvey Estuary.

2.4.2 Obtaining laser-derived length measurements – field methods

This study was licensed by the Department of Parks and Wildlife, WA (SF010738; CE005422), with all field work carried out in accordance to standards set by the Murdoch University Animal Ethics Committee (R2649/14). Use of the laser system was only permitted for personnel approved as competent or under the direct purview of an approved supervisor.

Between May 2016 and March 2017, boat-based surveys were conducted in Bunbury and Mandurah, while laser-derived data was collected in Shark Bay over a three-week period in October 2016, using both boat-based surveys and beach provisioning events. All boat-based

surveys were conducted using small research vessels (RV) less than 5.5 m in length, powered by 60-100 hp outboard engines.

When dolphin groups were sighted, dolphins were approached to within 5 m. Once with the group, location (Global Positioning System coordinates), behavioural, photo – identification and laser photogrammetry data were collected simultaneously until all individuals were photographed, with a minimum of five minutes spent with each group. To obtain useful photo-identification and laser photographs, the RV was positioned alongside targeted dolphin individuals, at approximate distances between 5 m and 25 m. When appropriate, photographs were taken of surfacing dolphin individuals, with the photographer using the camera autofocus point within the viewfinder to place the laser dots on the dolphin. Once sufficient photographs were captured or the decision was made to leave the group, the sighting was completed. Following the boat surveys, all photographed individuals were identified using population-specific photo-identification catalogues.

2.4.3 Age estimates for Bunbury and Shark Bay individuals

Photo-identification transect surveys have been conducted on the Bunbury *T. aduncus* population since 2007 (Sprogis *et al*., 2016), with additional *ad-hoc* data collection dating back to 1989. Individuals under the age of ten years consequently have higher-quality (more-precise) age estimations due to dedicated and focused survey effort. Minimum and maximum age estimates of dependent calves (approximately 0-3 years old) and independent juveniles (4-10 years old) were derived from long-term calf sighting and weaning date records. For those individuals first observed as adults, it was necessary to develop minimum age estimates. This was achieved by adding twelve years to the individual's estimated age, based on the notion that individuals of this species typically reach physical maturity within at least twelve years of age (Mead & Potter, 1990; Kemper *et al*., 2014). A pre-determined

maximum age value of 45 was assigned to individuals that were first sighted as adults, as this corresponds to accepted lifespan estimates for *T. aduncus* (Cockcroft & Ross, 1990).

Due to increased research effort over a longer temporal period, the age estimates of Shark Bay dolphin individuals are generally more precise and provided a wider range of age estimates. As part of Shark Bay Dolphin Project protocols, each age estimate was assigned to one of three accuracy categories, including: 'day' estimates that are accurate to within seven days; 'week' estimates that are accurate to within four weeks; and 'month' estimates where birth estimates fall within an accuracy of one year. For individuals with age accuracies greater than one year, first-sighting dates were used to set a minimum age, with a maximum age set at 45 years.

2.4.4 Data processing: Image selection procedure

Previous literature accounts and current error estimates were used to develop selection criteria for images taken in the field (Durban & Parsons, 2006; Rowe & Dawson, 2008; Leurs *et al*., 2015). Most studies cautioned against the influence of horizontal error, but researchers had to compromise during the image selection process by visually-and subjectively-selecting images where the target subject is oriented as close to perpendicular as possible.

To date, no means of accurately quantifying the horizontal angle within single-camera photographs have been developed, and as a result, rigorous image selection is considered to be best practice. For example, several studies have used only those photographs where the reader was confident that the angle was less than 10-20° from perpendicular (Durban & Parsons, 2006; Rowe & Dawson, 2008; Webster *et al*., 2010). Despite the fact this approach is commonplace among laser photogrammetry studies, only a handful of studies detailed the influence of horizontal angle on measurement error.

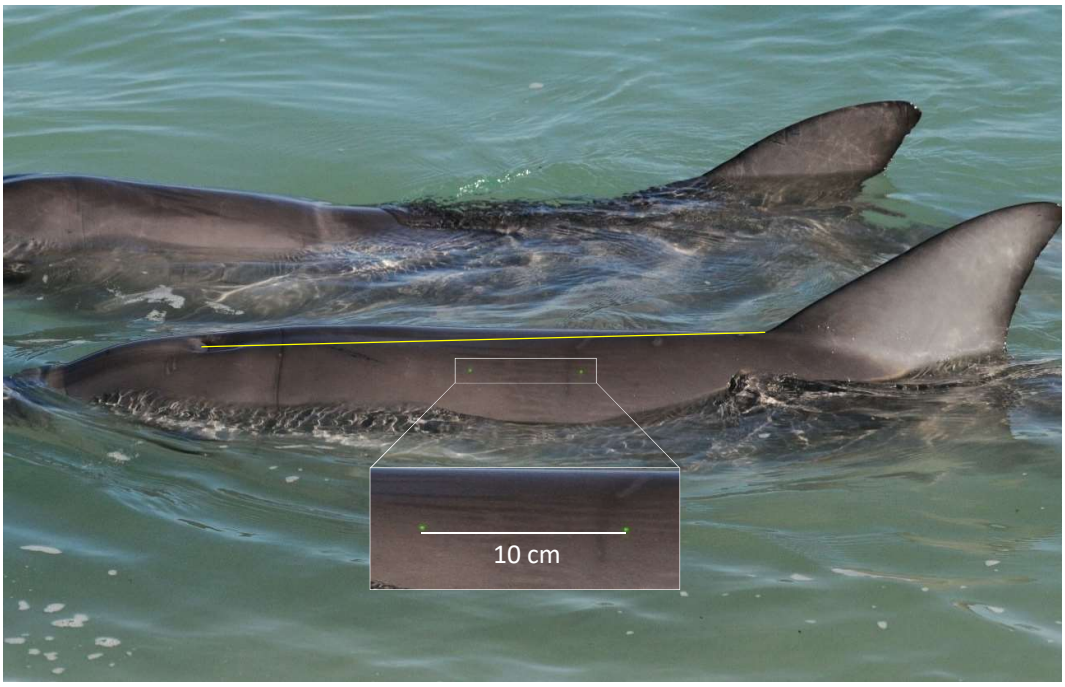

Figure 2.6 An example of a good quality photograph, with the dolphin positioned approximately perpendicular to the camera, displaying both the blowhole and origin of dorsal landmarks (yellow line joins the two) in addition to the two laser dots. The inset image provides an enlarged view of the two laser dots, calibrated at 10 cm apart.

In addition to displaying minimal angle, good quality photographs were required to be well lit and sharply focused, all the while displaying an unobstructed view of both laser dots positioned on the dorsolateral surface of the dolphin. In order to allow measurements to be taken, each photograph must display the full blowhole and dorsal fin of the target individual (**Figure 2.6**).

In most cases, photographs of the entire dorsal fin were obtained, allowing the individual to be identified using population-specific, photo-identification catalogues. Due to the high field effort in each of the study areas, it was possible to identify all subtle and well-marked individuals using body and dorsal fin markings unique to each individual (Wursig & Wursig, 1977). Images that satisfied the selection criteria were copied and stored separately from all other images taken on that day. The individual dolphins in these photographs were then identified, and the photograph renamed using the three-letter dolphin identification code and frame number.

2.4.5 Data processing: conversion of pixel counts into length measurements

Photographs which conformed to the selection process were measured using the free image processing software Image J (Rasband, 1997; https://imagej.nih.gov/ij/). Herein, the aim was to estimate the distance between the blow hole (BH) and the dorsal fin (DF) by using the 10-cm scale provided by the two green laser dots and information on the number of pixels within the image. Once imported into the software, a straight-line measurement quantified the number of pixels between the two laser dots. The pixel count over a 10 cm distance was then determined to set the measurement scale for the selected image. Because a wide range of lens magnifications were used during the study, no single 'global' scale was applied. By enlarging the image within the software *post-facto*, I accurately positioned the straight-line ruler between the medial point of the BH and the anterior insertion point of the DF (BH-DF; **Figure 2.7A**). Without a consistent and objective means of determining these positions, variations in placement across individuals could result in definition error (Durban & Parsons, 2006; Rowe & Dawson, 2008).

Determining the medial point of the BH was relatively simple because the structure is well defined and consistent between individuals, whereas positioning the anterior point of the DF was more subjective. In order to define the DF anterior insertion point, it was necessary to delineate the plane of the dorsal fin base by drawing a straight reference line that coincided with the main axis of the dolphin's back (**Figure 2.7B).** By then placing a line following the leading edge of the DF to the anterior base of the DF, the convergence point between the two reference lines indicated the anterior insertion of the DF (**Figure 2.7A**). This was confirmed by also following the plane of the dolphin's back towards the DF, and then identifying the point at which the angle deviated away from the back and into the leading edge of the DF. To maintain consistency, all measurements used in the study were made by myself.

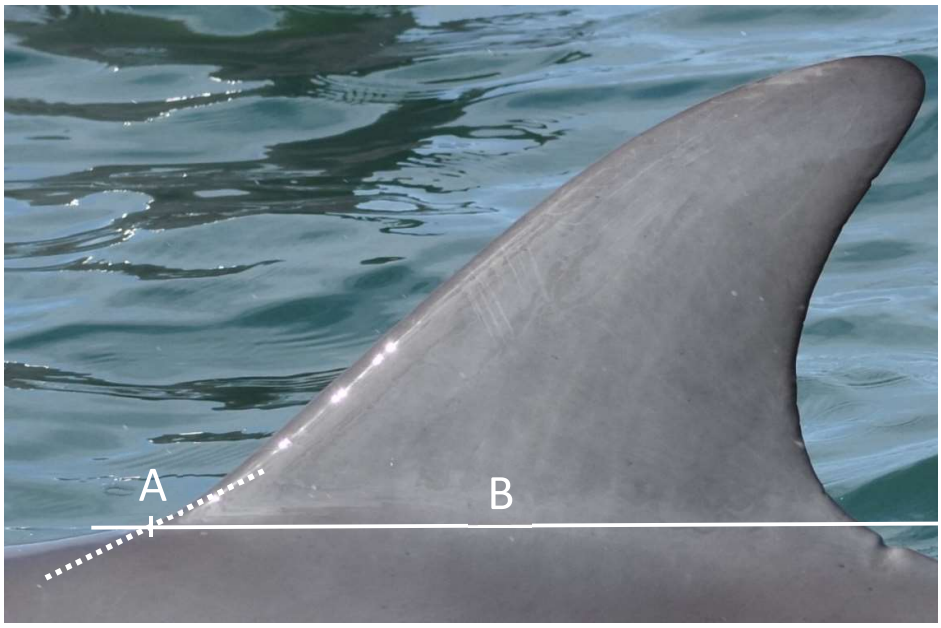

Figure 2.7 An example of the reference lines used to delineate the anterior insertion point of the dorsal fin (**A**). The dashed line represents the leading edge of the dorsal fin, while the solid line outlines the plane of the dorsal fin base (**B**).

2.4.6 Development of population growth curves for known-age populations

In order to describe the growth of *T. aduncus* in the two known-age locations, four common non-linear growth functions were applied to the observed length-at-age data (see equations below). The first two candidate models consisted of the 'typical' and 'original' forms of the von Bertalanffy growth function (von Bertalanffy, 1938). While these forms are similar, the former model considers time at zero (t_0) which represents the time or age when average length is zero, and therefore, has little biological meaning (Schnute & Fournier, 1980). The latter, however, is considered more appropriate for marine mammals and elasmobranch species that exhibit pre-natal growth, as length-at-birth (L_0) can be estimated following a gestational period (Cailliet *et al*., 2006). The final two candidate models include the Gompertz function (Ricker1 parameterization; Gompertz, 1825), as well as the Richards growth model, which is equivalent to the generalised von Bertalanffy function with the addition of a shape

parameter (Pauly, 1979), that enables the inflection point of the curve to be set anywhere between the range of minimum and maximum asymptote values. The respective equations for these growth functions are as follows:

- Original von Bertalanffy: $L_t = L\infty - (L\infty - L_0) * \exp^{(-K*t)}$
- Typical von Bertalanffy: $L_t = L\infty(1 - \exp^{(-K(t-t_0))})$
- Gompertz: $L_t = L\infty * \exp(^{-e(gi(t-t_0))})$
- Richards: $L_t = L\infty(1 - \exp^{(-K(t-t0))})^p$

Where L_t denotes length-at-age *t*,
$L\infty$ is the mean asymptotic BH-DF length,
K is the Brody growth rate coefficient, rate in attaining the asymptotic length
t_0 is the age at which size would be zero,
t is a theoretical function of time and age,
L_0 is the mean length at time zero (birth),
gi is the instantaneous growth rate at the inflection point; and
p determines the shape of the curve.

The candidate models were fitted using the 'FSA' package (Ogle, 2017) in R version 3.2.4 (R Core Team, 2013), with median parameter estimates and 95 % confidence intervals obtained through bootstrap resampling (1,000 iterations). The models were compared using Akaike Information Criterion (AIC; Akaike, 1974), and corrected delta AIC values (Δ) were applied to measure and rank each model relative to the best fitting model, using the 'AICmodavg' package (Mazerolle, 2015). As per Burnham and Anderson (2002), models with Δ= 0-2 had strong support, Δ= 4-7 had moderate, and Δ ≥ 10 minimal. Akaike model weights (AIC*w*), defined as the weight of evidence in favour of a specific model being most parsimonious from an available set of candidate models (Katsanevakis, 2006; English *et al.*, 2012), were then calculated to determine which of the four growth functions provided the best fit for length-at-age data attained in each location.

2.4.7 Sensitivity analysis: accounting for measurement and age estimation errors

It is important to investigate the extent to which error influences the quality of length-at-age estimates attained from chosen models, so that the models do not produce biased predictions that might lead to biological misinterpretations. In this case, potential errors can be attributed to both laser-derived length measurements as well as age estimation. Sensitivity analysis was conducted using the maximum error values for both laser-derived measurements and age estimation. The maximum measurement error estimate was obtained from the 3D replica experiment, using the maximum error value obtained at 15° from perpendicular (the greatest horizontal angle permissible in image selection). Maximum age calculations for each individual was used to profile the error associated with age estimation.

Bootstrap resampling methods were applied to calculate mean parameter estimates for the length-at-age models and their respective density distributions, by randomly resampling the laser-derived measurement (in cm) and age estimate (in years) of each individual by one thousand iterations and then re-fitting the best fitting growth model. From the density distributions, 95 % highest posterior density (HPD) intervals were calculated, which are equivalent to 95 % confidence intervals. Highest posterior density intervals are more appropriate for these analyses, due to the high number of resamples per individual (N=1,000 iterations) compared to the true sample size.

The bootstrapped resamples were then plotted to the best fitting growth curve, resulting in an 'error distribution' in the shape of a square around each data point, with the height and width of the square given by the measurement and error structure for each dolphin. These values, in combination with visual inspection of both the simulated growth curves and density distributions, were used to provide a measure of robustness of the growth curve model parameters.

2.4.8 Investigating morphological differences between populations

Several approaches were employed to test for morphological differences between Bunbury and Shark Bay. From the most parsimonious growth model identified, the asymptotic length of dolphins were compared between the two populations. In addition, the mean BH-DF length estimates was predicted for four age classes (year 1, 3, 12 and 25) and compared between the two populations, as these provided comparison across periods of both rapid growth and growth approaching an asymptote, while also accounting for regions where the asymptotic length has been reached on the selected growth curve. Years 3 and 12 also coincide with approximate major life history events for *T. aduncus*: weaning (Kemper *et al*., 2014) and the attainment of sexual-maturity (Mead & Potter, 1990) respectively. The confidence intervals (HPD distributions) around these mean length-at-age estimates were obtained from the bootstrapping procedure conducted during the sensitivity analyses. For example, the degree of overlapping between the two population distributions would indicate whether significant differences in BH-DF length were present for each age class. Finally, Welch Two Sample t-tests were carried out on each of the age classes, using the mean length-at-age estimates of each population as the dependent variable.

3. Results

3.1 Horizontal angle and distance

3.1.1 Two-dimensional calibration board experiment

The oscillating dial on the tripod allowed for an accurate estimation of angle increments throughout the entire 0-75° spectrum. A total of 240 non-sequential images of three images per angle and each distance increment were measured. The accuracy of the laser system was very dependent on the degree of the horizontal angle (**Figure 3.1)**.

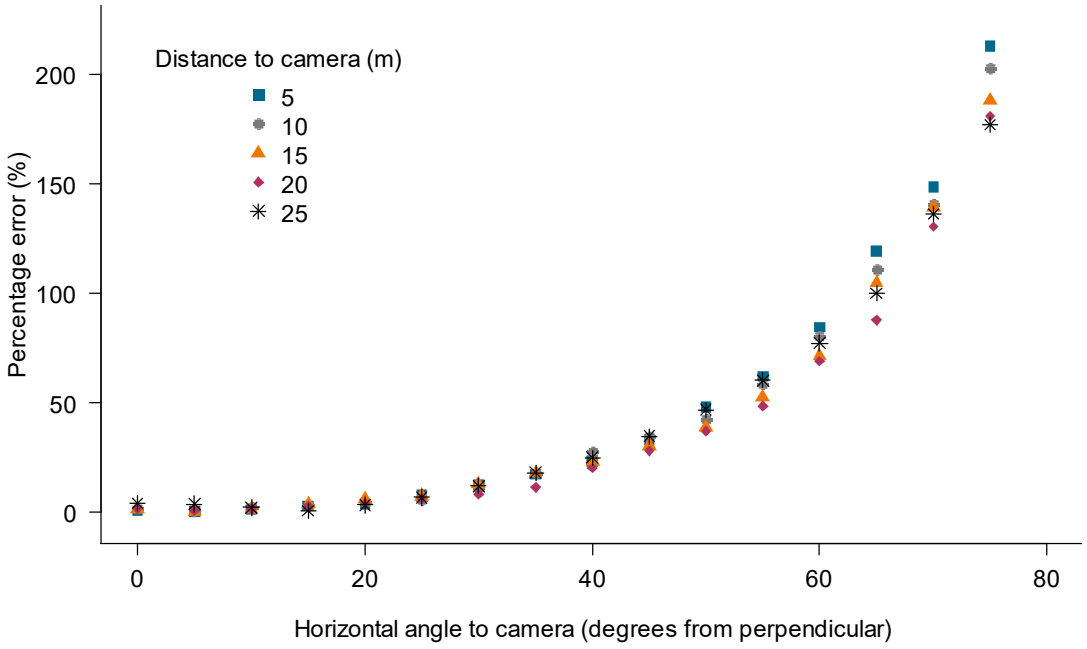

Figure 3.1 Plot exhibiting the results of the two-dimensional experiment, where horizontal angle was tested from 0° to 75°, using five distance increments (5-25m). Note the region of low measurement error at horizontal angles less than ~20°.

Angular deviations of up to 15° from perpendicular resulted in a mean error of 0.10 cm or 1.04 % of the known 10 cm distance. Laser-derived measurements were both under- and over-estimated, with estimated lengths between 9.63 and 10.35 cm. For horizontal angles

greater than 15°, there was a steady increase in the measurement error percentage ranging from 6 % to 50 % at 55°. Angles between 60° - 75° from perpendicular resulted in a larger variation of measurement errors, ranging between 70 % and 200 % respectively.

3.2 Body curvature

3.2.1 Replica model experiment

Three laser-derived measurements were averaged for each angle, distance and body zone (upper, middle, lower) increment, totalling 270 measurements. Measurement errors at deviations of <15° from perpendicular were comparable to the 2D calibration board experiment, with a mean error of 1.27 % (range= 0.02-6.21 %) or 0.81 cm (range= 0.02-3.84 cm). Horizontal angle had a significant effect on measurement values ($F_{5,\ 84}$ = 726.7, p < 0.001), while no differences were detected for either distance (p= 0.851) or curvature zone (p > 0.05).

Visual inspection of interaction plots suggested no interaction was present between the curvature zones and other variables (p > 0.1). However, an effect was detected between horizontal angle and distance, with a three-way ANOVA confirming the significant interaction ($F_{20,\ 60}$ = 2.461, p= 0.003). Since the assumption of homogeneity of variances was met, a *post-hoc* Tukey's honest significant difference (HSD) test was carried out. The interaction between horizontal angle and distance only became significant at angles ≥ 15°, with no significant between-distance differences found at angles < 15° (p > 0.3, mean difference =0.89 cm, range= 0.70-1.10). From all the tested angles, measurements obtained at 75° differed the most between distances (p < 0.01), with a mean difference of 2.10 cm (range= 0.97-3.04).

3.3 Difference between physical and laser-derived measurements

For each of the ten post-mortem subjects, straight BH-DF lengths were obtained using both physical and laser-derived measurements. For the laser-derived measurements, three non-sequential photographs of the post-mortem subjects were measured and averaged, totalling 30 measurements. There were no significant differences between the BH-DF lengths measured during post-mortem examinations and those derived by the laser photogrammetry technique (paired t-test: $t_9 = 1.522$, $p = 0.162$; see Table **3.1**). Since the horizontal angle was controlled during each examination, the measurement differences between the two techniques were minimal (mean= 0.55 %, range= -4.53-2.85 %), equating to a mean difference of 0.41 cm (range= -1.51-1.37 cm; see Table **3.1**).

Table 3.1 Summary of the ten post-mortem *T. aduncus* examined between May 2016 and April 2017. Individual demographic (age, sex) and measurement data (physical and laser-derived) are provided.

Dolphin Code	Age class	Sex	Fork TBL (cm)	Physical BH-DF (cm)	Laser BH-DF (cm)	Δ Laser Error %
CAB	MA	F	253.0	82.0	83.3	1.67
PIR	MA	F	249.0	80.5	81.1	0.74
HNA	MA	F	238.2	72.1	72.5	0.63
SWL	IJ	M	222.8	59.1	59.7	1.1
LDY	IJ	F	202.0	61.8	62.4	1.04
EST	DC	F	167.5	59.8	59.2	-0.95
BUN2	DC	M	135.5	43.5	44.7	2.85
PIRc	DC	M	134.1	44.1	45.0	2.24
AND	NEO	M	130.0	40.8	41.1	0.73
BUN1	NEO	M	102.0	33.3	31.8	-4.53
Mean	-	-	-	-	-	0.55

Notes: Age classes classified as MA= mature adult, IJ= immature juvenile, DC= dependent calf, and NEO= neonatal.
Sex as M= male and F= female.
TBL= total body length.
BH-DF= blowhole-to-dorsal fin length.

3.4 Relationship between blowhole-to-dorsal fin length and total body length

Straight measurements of both BH-DF and total body lengths (TBL) were obtained on ten post-mortem individuals, with distribution across all life stages (**Table 3.1**). There was a strong linear relationship between BH-DF and TBL, accounting for 92.2% of the variation in TBL ($F_{1,8}$ =107.2, p <0.001, R^2= 0.922, TBL= 3.16 X BH-DF; **Figure 3.2**).

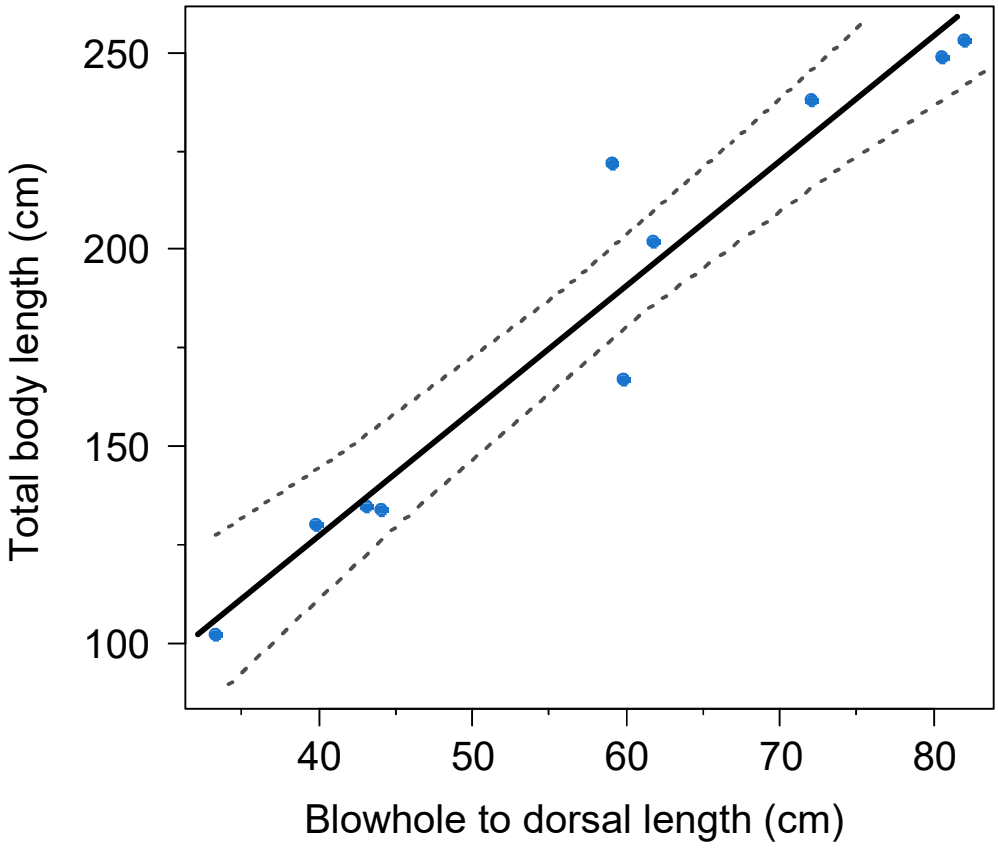

Figure 3.2 Relationship between total body length and the distance between blowhole and dorsal fin for Indo-Pacific bottlenose dolphins (*N*=10). The black line represents the fitted line of a linear model (TBL= 3.16 X BH-DF).

3.5 Applications of remote-laser photogrammetry: sample descriptions

3.5.1 Bunbury

Twenty-eight boat-based surveys were conducted between May 2016 and January 2017. Laser-derived measurements were obtained opportunistically during line-transect surveys (*N*=14), as well as dedicated 'laser' days (*N*=14). Of the 1,855 viable photographs displaying the lasers projected on the dolphin with clearly visible blowhole-to-dorsal-fin (BH-DF) landmarks, 715 satisfied the quality grading criteria (38.5 %).

A total of 103 individuals of minimum age were identified and measured, representing 24 males, 36 females, and 43 unknown-sex individuals (**Figure 3.3A**). Sex determination was only available for 8 % of individuals under the age of three, due to a lack of available sex data. Whereas long-term sex data was available for most Bunbury's catalogued sub-adults and mature individuals, reflected by a high (96 %) sex determination rate for individuals over the age of nine. Laser-derived measurements were obtained on individuals across all age classes, with minimum ages ranging from < 12 days to approximately 37 years.

Repeated measurements, defined as having two or more laser-derived BH-DF measurements, were available for 92 individuals (89 %) of the sampled population, with a mean of 5.88 measurements obtained per individual (range= 2-22 measurements). However, this mean was likely skewed due to outlier individuals having far more repeat measurements compared to others, suggesting the median of four repeat measurements per individual is more representative of the average number of measurements. A mean coefficient of variance (CV) of 2.03 % was estimated for repeated measurements of the same individuals across different photographs (range= 0.02-6.64 %).

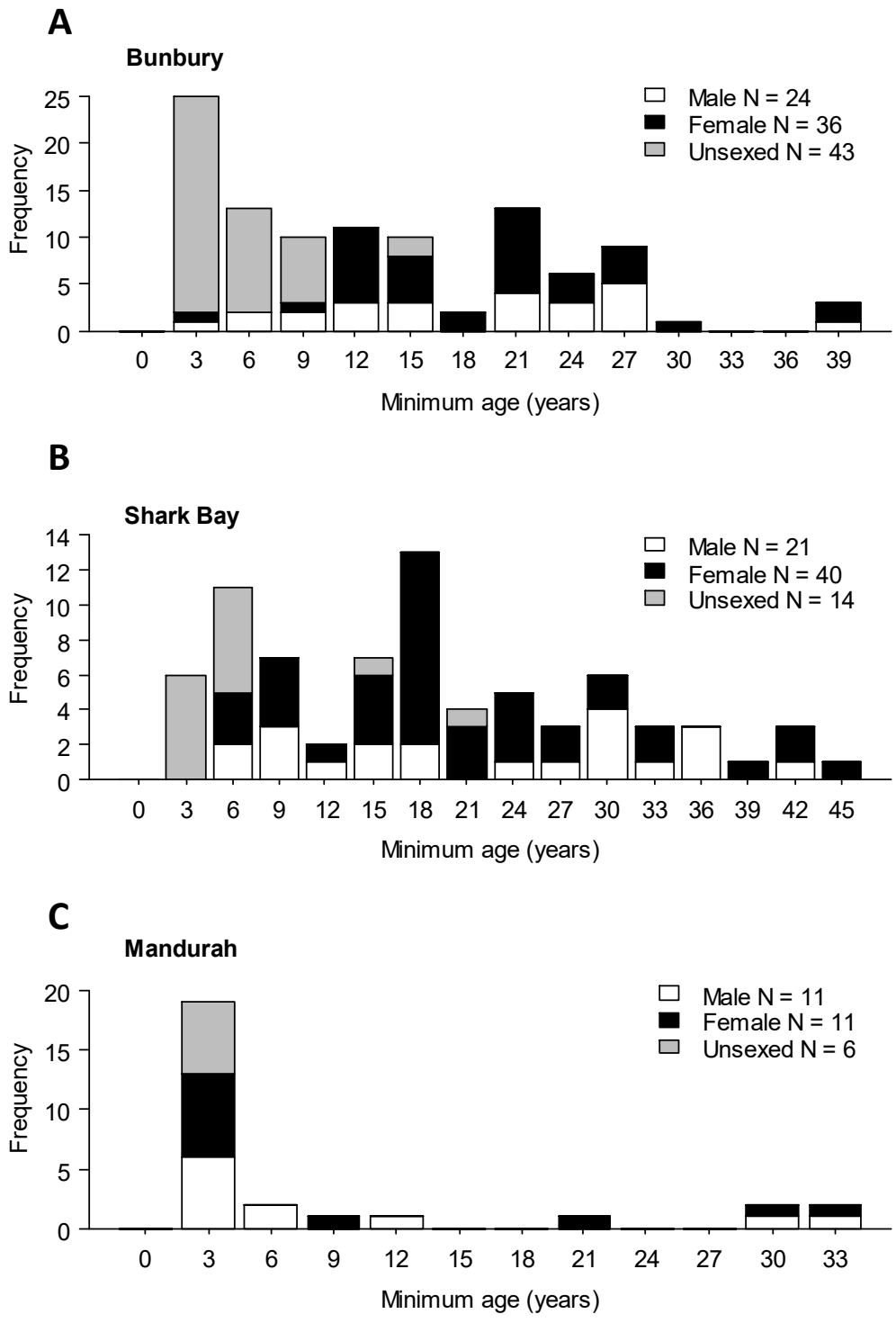

Figure 3.3 Age-frequency distributions of male (□), female (■) and unknown sex (■) *T. aduncus* sampled in Bunbury (**A**), Shark Bay (**B**) and Mandurah (**C**). Age bins represent the three years prior to the bin in question, e.g. the '3' age bin represents years 1 to 3.

3.5.2 Shark Bay

Laser-derived data was obtained over the first three weeks of October in 2016, utilising two data collection platforms: boat-based surveys (*N*=11) undertaken during favourable sea states and beach provisioning mornings (*N*=10) during poor weather. Over this period, 734 viable images (boat= 287, beach= 447) were captured, with 365 images (49%) satisfying the image selection process.

A total of 76 individuals were identified and measured following quality assurance procedures, with 21 males and nearly twice as many females (41; **Figure 3.3B**). Like Bunbury, sex data was limited for individuals < 6 years of age (29 %; **Figure 3.3B**) while sex data was available for 96 % of measured individuals over the age of 12. A wide range of minimum ages were sampled in Shark Bay, with the youngest individual confirmed to be < two weeks of age, and the oldest >40 years.

Repeated measurements were available for 56 individuals, equating to 74 % of the sampled population. Individuals sampled during beach provisioning events were photographed more frequently compared to those sampled during boat surveys, resulting in a wide distribution of repeat measurements (range= 2-39; median= 4). Mean CV estimates were smaller in Shark Bay than in Bunbury (CV= 1.69 %, range= 0.03-8.8 %).

3.5.3 Mandurah

Eight boat surveys were conducted in Mandurah between June 2016 and March 2017. A total of 210 images passed grading, resulting in 28 known-age dolphins being sampled (**Figure 3.3C**). Repeated measurements were available for 22 individuals (79 % of sampled population, range=2-15, median=5), resulting in a mean CV estimate of 1.83 % (range=0.09-6.08 %). The youngest sampled individual was < four days old, and the oldest > 30 years (Figure **3.3C**).

3.6 Applications: development of population growth curves

3.6.1 Growth model selection

All four candidate growth models were successfully fitted to age-at-length data of each population. Of the four growth models fitted, the Richards growth function (RGF) attracted the strongest support in describing *T. aduncus* growth in all sampled populations (**Table 3.2**). For the Bunbury and Mandurah datasets, the RGF was assigned the highest possible weighting value (AIC*w*= 1.00), while others received an AIC*w* of zero, suggesting it provided the best fit by far. For Shark Bay, however, the RGF received only moderate support (AIC*w*= 0.50), with evidence to suggest both the typical (TvB) and original (OvB) von Bertalanffy models also fitted the data reasonably well (**Table 3.2**). Visual inspection of the growth models confirmed this, with greater overlapping of the models in Shark Bay compared to Bunbury and Mandurah (see **Figure 3.4B**). The Gompertz (GOM) function was the least parsimonious model for all three sampled populations.

Table 3.2 Summary of Akaike's information criterion (AIC) model selection output for the four candidate growth models: the Richards (RGF), original von Bertalanffy (OvB), typical von Bertalanffy (TvB) and Gompertz (GOM), used to describe the BH-DF length-age relationship for *T. aduncus*. The most parsimonious model for each Indo-Pacific bottlenose dolphin population is highlighted in bold.

Population	Candidate model	AICc	Δ AICc	AIC*w*	Log Likelihood
Bunbury	**RGF**	**540.74**	**0.00**	**1**	**-265.06**
	OvB	555.44	14.70	0	-273.51
	TvB	555.44	14.70	0	-273.51
	GOM	557.62	16.88	0	-274.61
Shark Bay	**RGF**	**355.68**	**0.00**	**0.50**	**-172.40**
	OvB	357.26	1.58	0.22	-174.34
	TvB	357.26	1.58	0.22	-174.34
	GOM	360.04	4.37	0.06	-175.74
Mandurah	**RGF**	**170.30**	**0.00**	**1**	**-78.79**
	OvB	183.12	12.82	0	-86.69
	TvB	183.12	12.82	0	-86.69
	GOM	184.98	14.68	0	-87.62

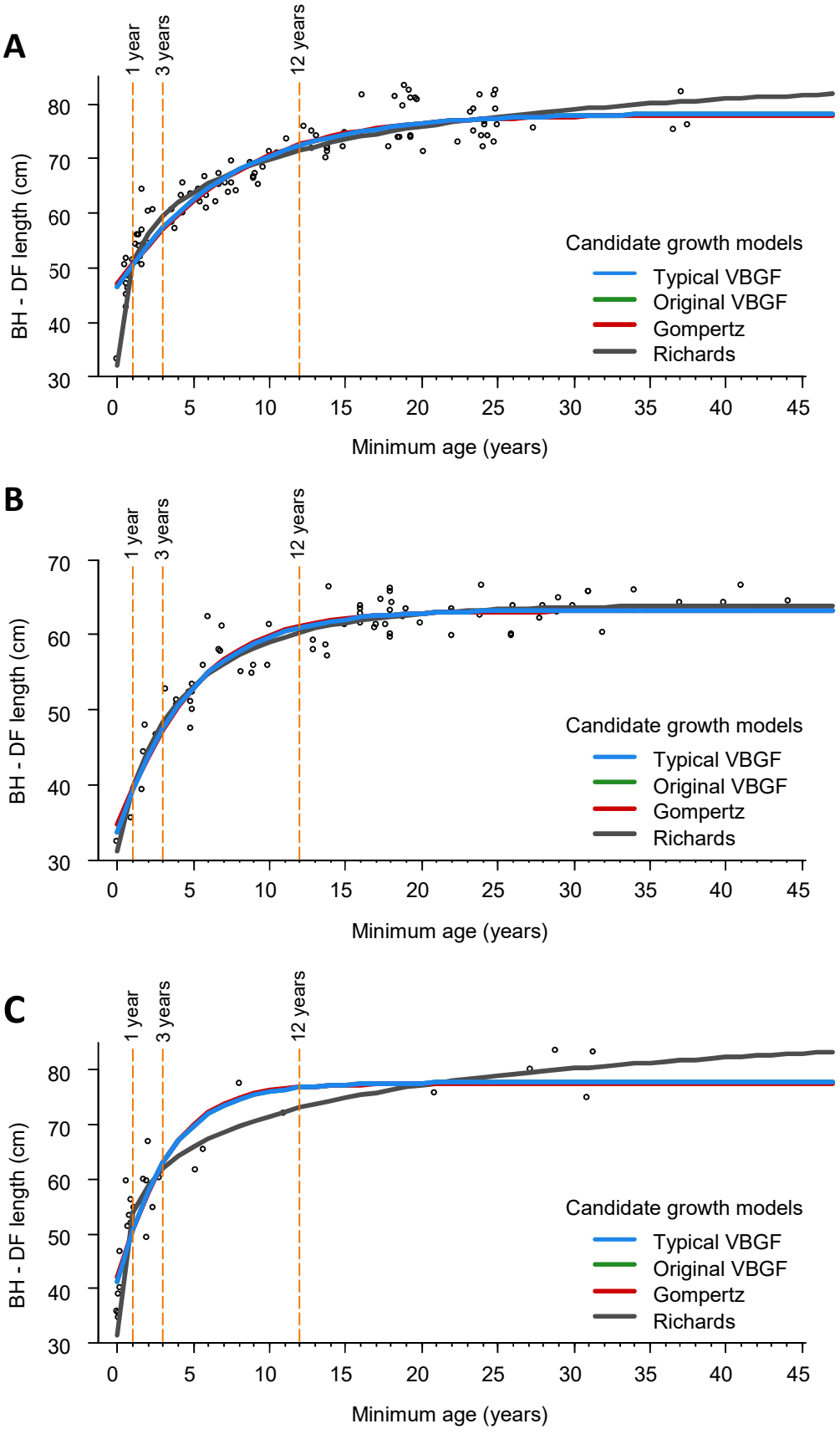

Figure 3.4 Visual representation of each of the model fits (see legends) relative to the length-at-age data obtained for each population (Bunbury, **A**, *N* = 103; Shark Bay, **B**, *N* = 75; Mandurah, **C**, *N* = 28).

3.6.2 The estimation of biological parameters from selected growth models

No clear sexual dimorphism was evident in any of the sampled populations, therefore all sampled individuals were pooled for growth curve analyses. Despite being the most parsimonious model for both Bunbury and Mandurah populations, the RGF had difficulty converging during the parameter estimation procedure. While the RFG model fitted the observations closely, the output parameter values for asymptotic length was unrealistic from a biological aspect. (**Table 3.3**). For Shark Bay, however, it was possible to obtain meaningful RGF parameter estimates, due to improved model fit. For additional inference, the output parameters from the second-most parsimonious model – the OvB function – were also analysed, with the aim of attaining improved estimates of asymptotic length in addition to length-at-birth.

3.6.3 Description of calf length-at-birth and postnatal growth

Due to a lack of data points between 30 and 40 cm, mean length-at-birth (L0) estimates for Bunbury were overestimated at 46.38 cm and unlikely to be reliable. A neonatal specimen was measured during a necropsy examination and was confirmed to be less than ten days old, due to the presence of a prominent urachus (remnant channel linking the bladder and umbilicus; N. Stephens, Murdoch University, *pers comm.* July, 2016). This Bunbury male was separated from its unknown mother and subsequently euthanized. Since this individual was deemed to be in good physical condition, its BH-DF length of 33.57 cm was deemed representative and therefore included in L0 inferences. While the sex of sampled neonatal calves in Mandurah and Shark Bay are unknown, excellent age estimates were available for individuals measured close to birth, providing L0 estimates of 34.38 cm and 32.02 cm respectively **(Table 3.3).**

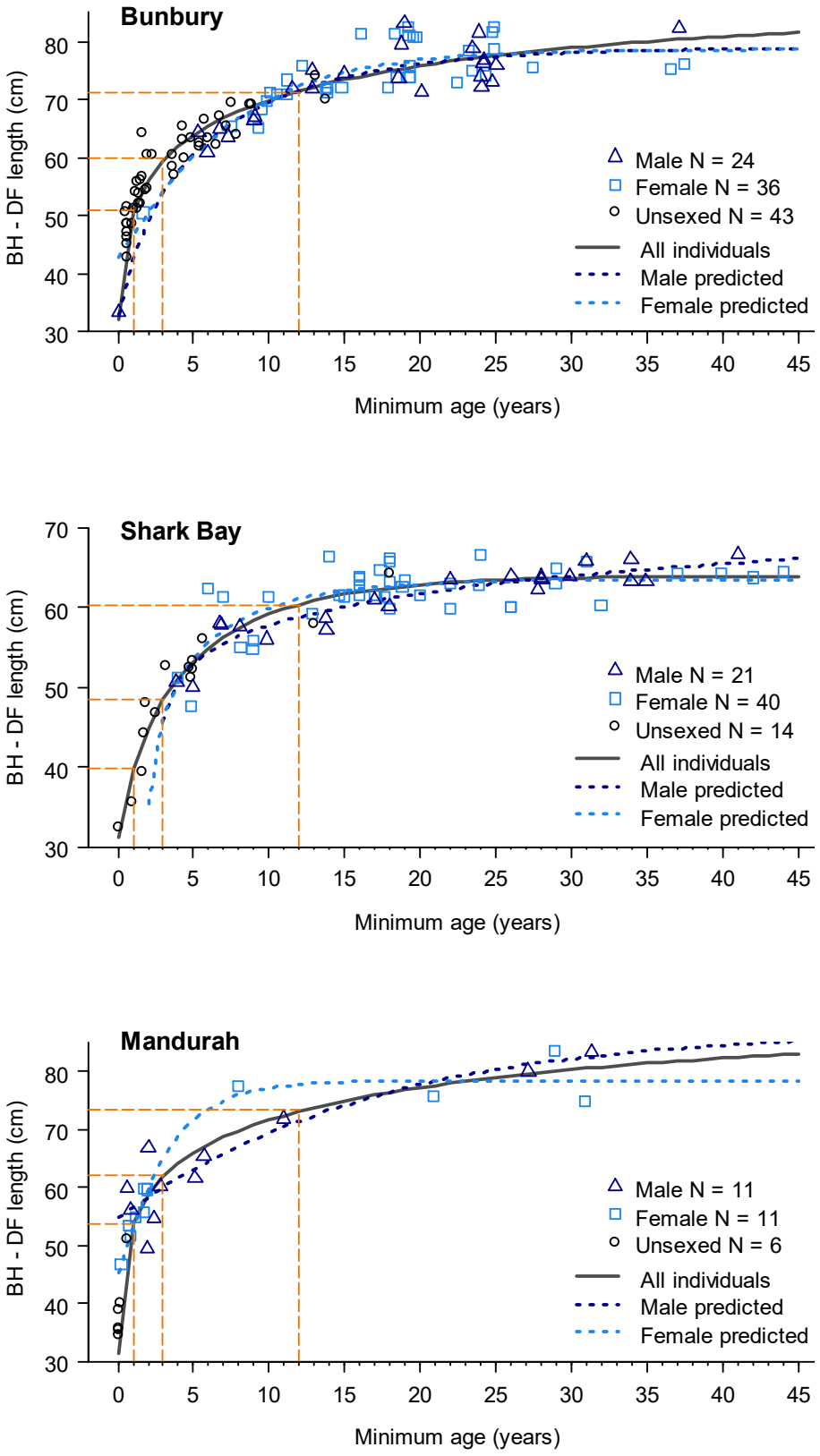

Figure 3.5 Combined-sex Richards growth curves (—) for *T. aduncus* sampled in Bunbury, Shark Bay and Mandurah study sites. Male (△), female (□), and unknown sex (o) dolphins are plotted, along with sub-setted male (- -) and female (- -) lines. Reference lines (- -) have been added to highlight the inflection point at various years of age: 1, 3 (weaning) and 12 (age at maturity).

Table 3.3 Summary of median asymptotic length (L∞), length-at-birth (Lo) and growth rate constant (*K)* parameter estimates for the Richards (RGF) and original von Bertalanffy (OvB) growth functions. Both the growth models were sub-setted to investigate male (M), female (F), unknown-sex (U) growth separately, as well as for all individuals combined (A).

Population	Sex	*N*	Growth Model	L∞ (95 % CI) (cm)	Lo (95 % CI) (cm)	*K* (95 % CI) ($year^{-1}$)
Bunbury	M	24	RGF	79.08 (76.08-FC)	-	0.11 (FC-FC)
			OvB	77.73 (75.72-80.19)	33.57 (28.40-40.32)	0.17 (0.13-0.22)
	F	36	RGF	78.74 (76.75-81.56)	-	0.16 (0.11-0.22)
			OvB	79.00 (76.91-82.14)	41.38 (33.53-50.32)	0.14 (0.09-0.19)
	U	43	RGF	FC	-	FC
			OvB	FC	45.33 (42.12-47.87)	0.26 (0.15-0.41)
	A	103	RGF	85.32 (79.57-FC)	-	0.03 (0.00-FC)
			OvB	78.35 (76.77-80.45)	46.38 (44.43-48.31)	0.14 (0.11-0.17)
Shark Bay	M	21	RGF	FC	-	FC
			OvB	66.48 (64.17-FC)	FC	0.06 (0.02-0.12)
	F	40	RGF	63.5 (FC-FC)	-	0.16 (FC-0.39)
			OvB	63.35 (62.20-65.18)	34.24 (FC-FC)	0.21 (0.10-0.40)
	U	14	RGF	62.88 (58.84-FC)	-	0.17
			OvB	61.52 (58.62-65.97)	32.02 (28.71-35.5)	0.26 (0.18-0.36)
	A	75	RGF	63.97 (63.02-65.63)	-	0.13 (0.08-0.21)
			OvB	63.34 (62.57-64.20)	33.73 (30.58-37.11)	0.21 (0.17-0.25)
Mandurah	M	11	RGF	86.80 (76.74-FC)	-	0.07 (0.00-0.18)
			OvB	FC	FC	FC
	F	11	RGF	78.39 (75.93-80.99)	-	0.36 (0.23-0.50)
			OvB	78.48 (76.21-81.32)	44.66 (40.17-49.04)	0.30 (0.19-0.43)
	U	6	RFG	FC	-	FC
			OvB	FC	34.38 (33.07-35.54)	FC
	A	28	RGF	88.12 (FC-FC)	-	0.02 (FC-FC)
			OvB	77.75 (73.72-82.17)	41.20 (37.21-45.41)	0.30 (0.19-0.44)

FC, value where the growth model failed to converge, resulting in no parameter estimate.

As expected, early regions in each of the population curves were characterised by rapid growth before stabilising as individuals approached maturity (**Figure 3.5**). Differences in early growth were present between locations. In Bunbury and Mandurah, it appears young calves experience a distinct growth spurt over the initial six months of life, before slowing down considerably as they approach their second year and weaning around the age of three. This is demonstrated by the near-vertical growth presented in **Figure 3.5A; C**). This region of the growth curve was problematic when fitting the growth models, with only the flexible RGF providing a good fit **(Figure 3.5A).** This accelerated growth was not detected for Shark Bay calves, reflected by improved fit from all candidate models. Moreover, this slowed growth is linear throughout the juvenile and sub-adult years, which allowed for improved fitting of all the candidate models during this period **(Figure 3.5B).**

3.6.4 Description of asymptotic growth

The combined-sex (male, female, unknown-sex pooled) RGF failed to reach a clear asymptotic length ($L\infty$) for the Bunbury population, with growth continuing as individuals approach maximum age (**Figure 3.5A**), reflected by overestimated asymptotic values in **Table 3.3**. However, the asymptotes for both the male and female RGF curves were more stable, producing comparable $L\infty$ estimates, with BH-DF $L\infty$ lengths of 79.08 cm and 78.74 cm respectively. The male, female and combined-sex OvB models also produced similar $L\infty$ estimates for Bunbury, see **Table 3.3**. Due to a combination of low sample size and the presence of outlier individuals, $L\infty$ estimates for Mandurah vary by sex and growth model, with no realistic asymptotic information available for the male and unknown-sex curves (**Table 3.3; Figure 3.5C**). However, $L\infty$ values estimated by the female and combined-sex RGF and OvB models were very close to those of Bunbury, with mean $L\infty$ estimates of 78.37 cm and 79 cm respectively.

Again, the Shark Bay data was well described by the RGF and OvB candidate models (**Figure 3.4B**), resulting in robust L∞ estimates in (**Table 3.3**). Combined-sex L∞ estimates were consistent between the two growth models, with the RGF and OvB models estimating 63.97 cm and 63.34 cm respectively. Possible sexual dimorphism was detected by the OvB, with a male L∞ estimate of 66.48 cm and 63.5 cm for females. However, overlapping confidence intervals suggest that this is not a significant difference.

3.6.5 Accounting for age and measurement error: sensitivity analyses

The increased horizontal length of these error distributions demonstrates higher uncertainty of age estimations, while the height indicates the maximum laser-derived measurement error recorded at 15° in the 3D replica experiment. While the error figure obtained in the replica experiment was 1.27 %, a larger value of 2 % was used to provide greater certainty.

The size of these error distributions was greatest for Bunbury individuals over the age of 20, with improved certainty for younger individuals (**Figure 3.6**). Age estimations of Shark Bay individuals are of better quality, indicated by the reduced size of error distribution across the age spectrum, with only greater uncertainty present in individuals estimated over the age of 30 years. While these error distribution representations should not be ignored, the sensitivity of the bootstrapped RGF curves to such variability will provide insight into the robustness of the selected RGF model. Following the resampling procedure, the form of both the Bunbury and Shark Bay RGF curves remained relatively unchanged, with no significant deviations from the original RGF curve, providing evidence of model robustness (**Figure 3.6**).

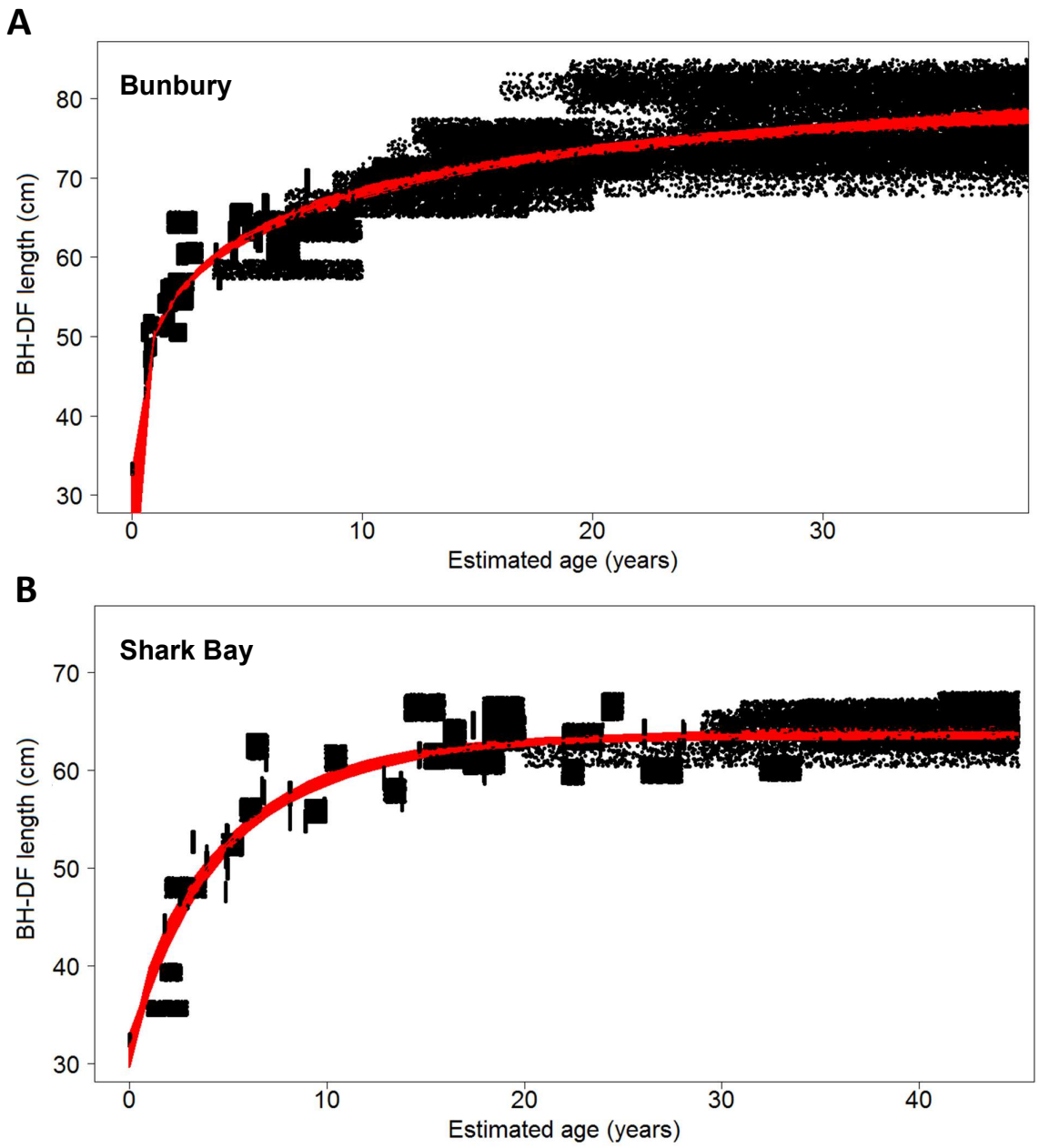

Figure 3.6 Visual representations of the bootstrapped error distributions characterising the relative measurement and age estimation error associated with each individual sampled in Bunbury (**A**) and Shark Bay (**B**). Bootstrapped Richards growth function curves are also displayed in red. Note the increased size of the error distributions for mature Bunbury individuals with relatively less error present in younger individuals.

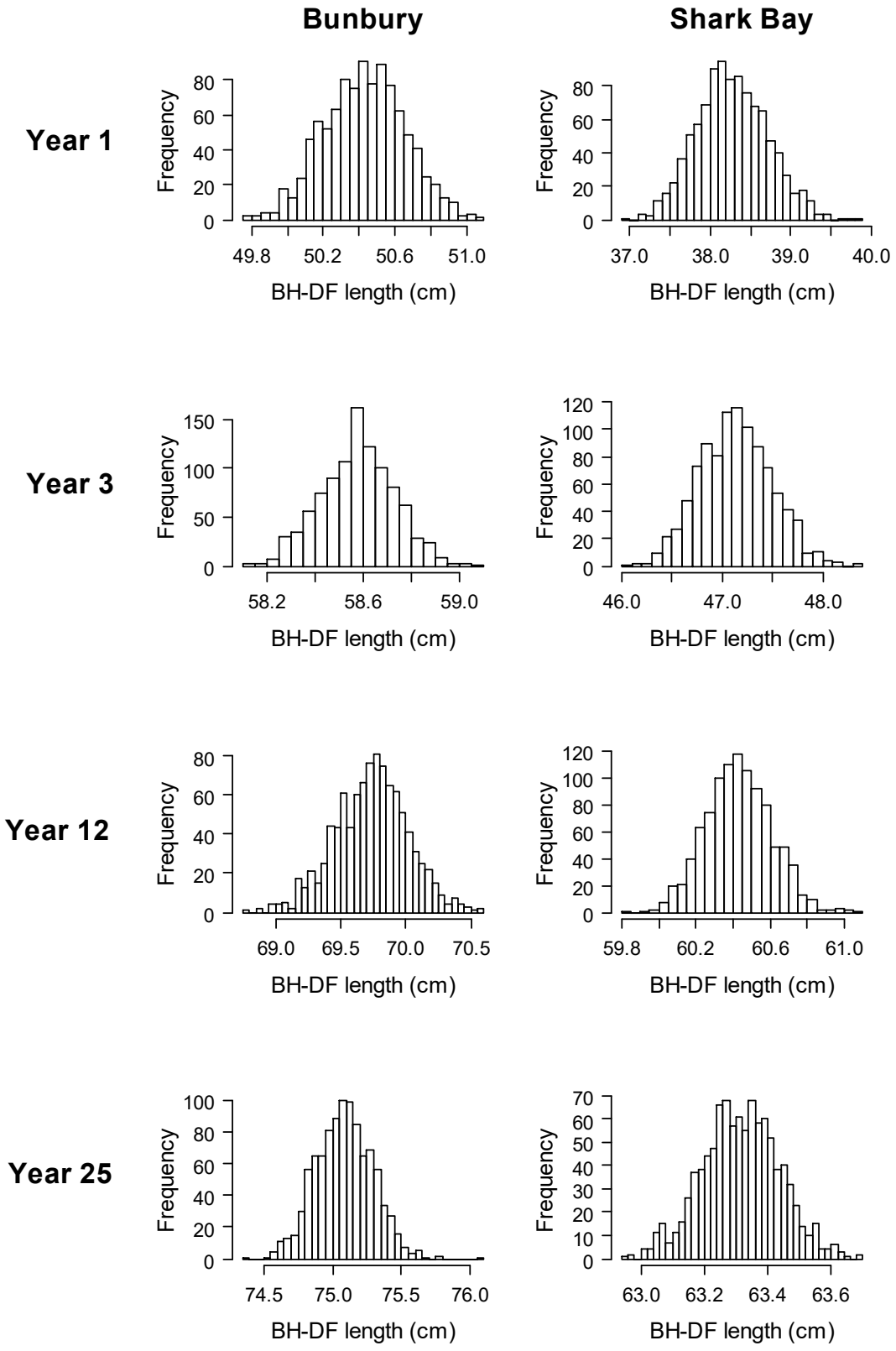

Figure 3.7 Frequency distributions representing the density distributions around the bootstrapped length-at-age values between Bunbury and Shark Bay. Differences in blowhole-to-dorsal fin length (BH-DF) were tested using four age classes: years 1, 3, 12, and 25.

Each of the estimated length-at-age values in Bunbury and Shark Bay displayed relatively narrow distributions following the bootstrapping procedure, suggesting the RGF model was not easily influenced by the error sources present in this study (**Figure 3.7**). This narrow distribution is echoed by the tight higher posterior density (HPD) intervals reported in **Table 3.4**. The laser-derived measurement error obtained from the 3D replica experiment was then increased from 2 % to 5 %, with no significant differences (paired t-test, $p > 0.05$) detected between the mean length-at-age estimates.

Table 3.4 Mean length-at-age estimates derived from the sensitivity analyses, with 95 % HPD values included. Age-specific population differences in BH-DF lengths and their respective Welch Two Sample t-test p values are included. Length at age x is represented as Lx, for example length at year 1= L1.

Population	L_1 (cm) (95 % HPD)	L_3 (cm) (95 % HPD)	L_{12} (cm) (95 % HPD)	L_{25} (cm) (95 % HPD)
Bunbury	50.43 (50.04-50.84)	58.58 (58.33-58.88)	69.74 (69.24-70.27)	75.08 (74.71-75.47)
Shark Bay	38.28 (37.49-39.57)	47.13 (46.46-47.87)	60.43 (60.08-60.79)	63.31 (63.09-63.57)
Δ BH-DF (cm)	12.16 (12.12-12.19)	11.45 (11.43-11.46)	9.31 (9.29-9.33)	11.77 (11.75-11.78)
df	2.93	2.67	3.40	3.40
T value	22.87	26.42	26.13	26.13
p value	< 0.001	< 0.001	< 0.001	< 0.001

3.6.6 Investigating morphological differences between intra-specific populations

The most parsimonious growth model – the RGF – was used to determine whether the *T. aduncus* populations in Shark Bay and Bunbury differed in morphology. However, due to a lack of model convergence in the Bunbury RGF, it was not possible to use the RGF output parameters (L_∞, Lo, *K*) for population comparison.

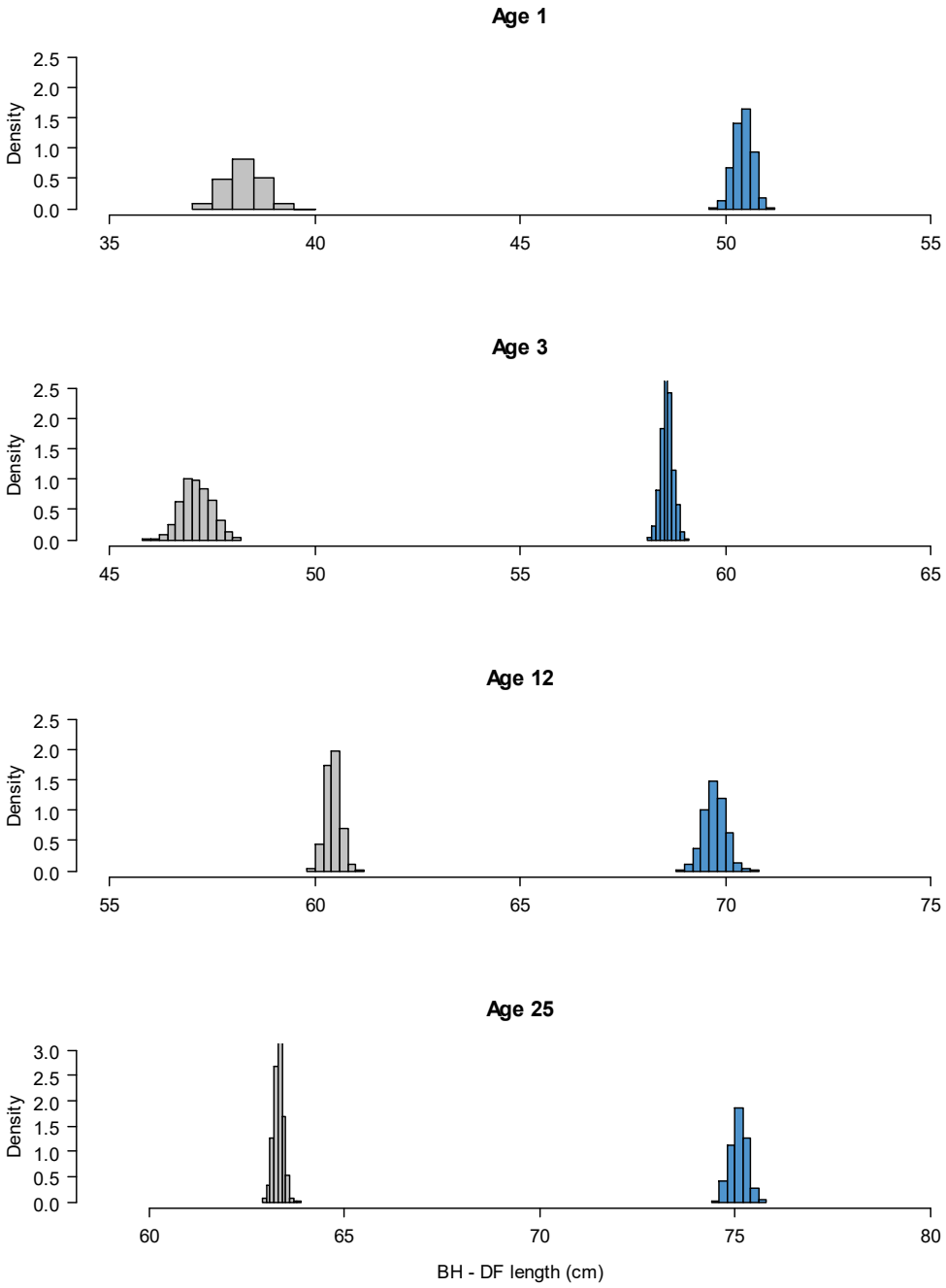

Figure 3.8 Bootstrapped density distributions of parameter values of the RGF growth model fitted to length -at -age data from Bunbury (blue) and Shark Bay (grey) individuals across the four tested age classes. Note the significant differences in BH-DF length demonstrated by a lack of overlapping distributions.

Instead, bootstrapped length-at-age estimates derived from the RGF were compared using the four age classes applied during the sensitivity analyses. Predicted BH-DF lengths for ages 1, 3, 12 and 25 differed significantly between Bunbury and Shark Bay individuals (Welch Two Sample t-tests specific to each age class, $p < 0.001$). There were population differences in mean BH-DF length across the four age classes, with an average BH-DF length difference of 11.17 cm (range 9.31-12.16 cm). The distributions of these values were plotted by age class, with the respective population distributions overlaid on the same plot to visually determine whether the HPD intervals overlap (**Figure 3.8**). The significant differences in mean length-at-age are confirmed by the non-overlapping distributions present in each of the age classes.

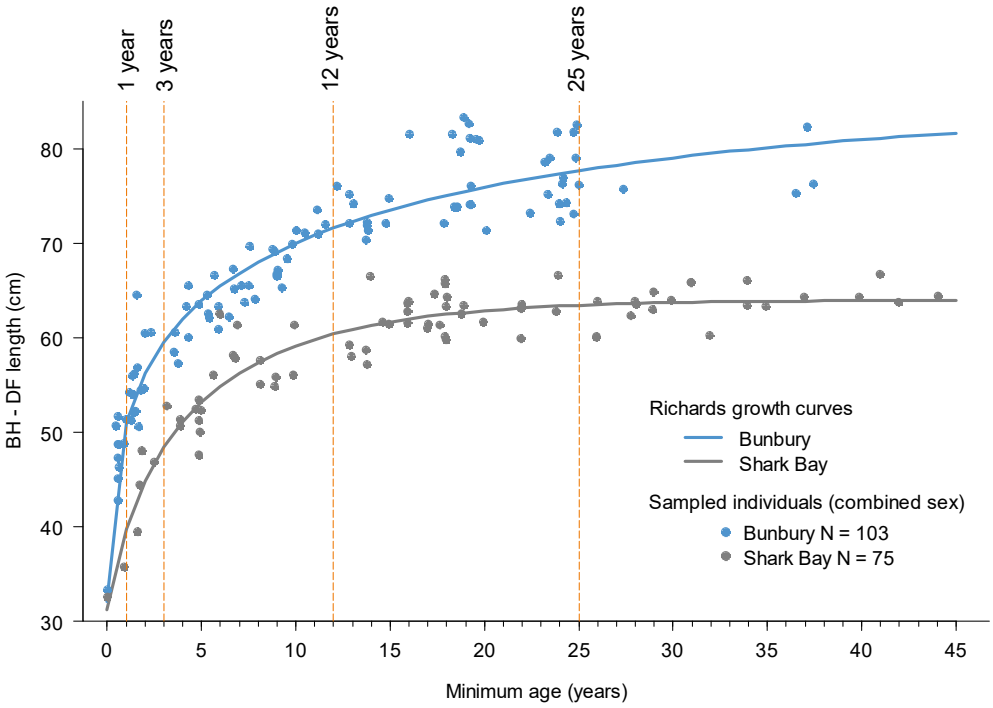

Figure 3.9 Overlaid Richards growth function (RGF) curves for Bunbury (—) and Shark Bay (—) demonstrating the differences in length-at-age measurements of sampled individuals. Note the lack of overlapping data points between the two populations.

Visual inspection of the two population RGF curves demonstrate the marked differences in BH-DF for individuals of the same age (**Figure 3.9**). One of the clear differences between the two population curves was in first year growth, where the difference in bootstrapped BH-DF length-at-age means was 12.16 cm (Bunbury: 50.43 cm, HPD: 50.04-50.84 cm; Shark Bay: 38.28 cm, HPD: 37.49-39.57 cm; **Table 3.4**). The Bunbury RGF predicted much steeper growth over the first six months compared to the Shark Bay RGF (**Figure 3.9**).

4. Discussion

4.1 Study overview

This study clearly demonstrates the feasibility and potential of remote laser photogrammetry as a non-invasive tool for obtaining morphometric measurements of free-ranging cetaceans. It is the first study of its kind in Australia, and provides valuable morphometric measurements of Indo-Pacific bottlenose dolphins in Bunbury, Mandurah and Shark Bay, Western Australia. Potential sources of error in the technique were detected by measuring models of known size and investigating how error varied in relation to distance from the subject, body curvature as well as the degree of rotation (horizontal angle).

When obtained at appropriate horizontal angles (i.e. <15° from perpendicular), photographs provided reliable blowhole-to-dorsal fin (BH-DF) length measurements, as illustrated by the respective error experiments. It was then possible to develop population growth curves for the three study sites and compare morphological differences between geographically isolated populations, providing the basis for investigations into the potential ecological factors driving growth and morphology.

4.2 Feasibility of laser photogrammetry as a morphometric technique

4.2.1 Sources of error and their influence on measurement accuracy

The findings from the flat board and dolphin replica experiments demonstrate the influence of horizontal angle on measurement accuracy. Ultimately, measurements obtained at horizontal angles greater than 15° from perpendicular were considered inaccurate. The measurement error values obtained at angles less than 15° were, however, well within the range of error values reported from similar experiments. For example, the error value achieved in the current study was 1.27 %, while similar horizontal angle experiments

conducted by Leurs *et al*. (2015), Rohner *et al*. (2016) and Webster *et al*. (2010) all yielded measurement error values between 1.2 % and 3.5 %.

As expected, increases in distances between the laser system and study subjects did not result in any significant measurement error when tested at a perpendicular angle. This is because the two points projected from the parallel lasers are considered equidistant (when calibrated), meaning the distance between the two projections remain constant regardless of the distance (Rothman *et al*., 2013). However, the equidistant relationship was disrupted at angles greater than 15° from perpendicular, with a significant interaction effect detected between horizontal angle and distance. This finding should, therefore, prompt greater caution during the image selection process.

To my knowledge, no other photogrammetry study has investigated the potential influence of convex body curvature on laser-derived measurement accuracy. No significant differences in BH-DF measurement values were detected between the designated dorsal, dorso-ventral and ventral zones of both post-mortem subjects and the replica model. This was consistent throughout each of the horizontal angle and distance increments, which indicates a lack of interaction between the three error variables. This finding suggests that the position of the laser points along the vertical axis of the curved dolphin skin surface does not influence measurement accuracy, and therefore, was not included in the image selection procedure subsequently.

4.2.2 Difference between physical and laser-derived measurements

Access gained to ten post-mortem individual bottlenose dolphins permitted direct comparison between physical and laser-derived BH-DF measurements. No significant differences were detected between the two measurement techniques, with a low mean measurement error of 0.41 cm (0.55 %). It is important to note, however, the conditions in which these measurements were attained were highly controlled. In essence, the low error

reported in this experiment should serve as an example of the greatest accuracy the laser photogrammetry technique can achieve when external conditions such as horizontal angle are accounted for.

4.2.3 Degree of precision achieved using laser photogrammetry

The level of measurement precision achieved using laser photogrammetry was evaluated by comparing the variation between the measurement values obtained from different photographs of the same individual. For all three sampled populations, the mean coefficient of variance (CV) values were ~ 2 % or less, which compared favourably with the CV values reported in previous cetacean photogrammetry studies. For example, Webster *et al*. (2010) applied laser photogrammetry to measure the dorsal fin base length and fin height of free-ranging Hector's dolphins (*Cephalorhynchus hectori*), and reported CV values of 3.71 % and 3.76 % respectively. For sake of comparison, stereo-photogrammetry techniques derived mean CV values of 4.38 % when measuring BH-DF lengths in sperm whales (*Physeter macrocephalus*; Dawson *et al*., 1995). Aerial photogrammetry studies also yielded median CV values < 2 % for total body length measurements of both Antarctic killer whales (*Orcinus sp.*; Pitman *et al*., 2007) and southern right whales (*Eubalaena australis*; Best & Ruther, 1991). The relatively low mean CV values achieved in the current study supports the notion that consistency had been achieved with my calibrated laser system, and that this also extended to both the image selection and measurement procedures.

4.3 Relationship between blowhole-to-dorsal fin length and total body length

Obtaining total length measurements of free-ranging cetaceans in a non-invasive manner is difficult if not near-impossible, without the use of aerial photogrammetry or morphometric indices that can be used as proxy measurements for total body length. In the current study, linear regression provided evidence of a strong positive relationship between BH-DF length and total body length (TBL) in *T. aduncus* (N=10; R^2= 0.92). This relationship has also proven

to be strong for other odontocete species including sperm whales (*Physeter macrocephalus*; Dawson *et al*., 1995), Hector's dolphins (*Cephalorhynchus hectori*; Brager & Chong, 1999), and common bottlenose dolphins (*Tursiops truncatus*; Cheney *et al*., 2015).

This relationship is important because obtaining TBL estimates on free-ranging cetaceans is not practical, as they only expose their back (dorsal region) when they break the water surface. While this can be negated using aerial photogrammetry (Fearnbach *et al*.,2011), morphometric indices such as BH-DF length are emerging as suitable proxy measurements. Moreover, the use of laser photogrammetry suits this scenario well, as the laser projections can easily be placed between the blowhole and dorsal fin, resulting in cheaper, more efficient TBL estimates.

Traditionally, morphometric studies on cetaceans utilise TBL measurements to investigate geographical morphotypes (Murphy & Rogan, 2006), health and fitness (Hart *et al*., 2013), as well as the inference of life-history parameters such as length at sexual maturity (Perryman & Lynn, 1993). Therefore, while BH-DF measurements are not extensively used in morphometric studies currently, there is potential to convert these measurements into TBL lengths, where a greater number of direct length comparisons between groups (e.g. populations, sexes) can be made using both previous and future studies.

4.4 Developing growth curves for well-studied dolphin populations

4.4.1 Selection of growth curve models

Studies aiming to characterise the length-at-age growth of free-ranging animals generally apply and compare more than one sigmoidal growth functions (Katsanevakis, 2006; Piercy, Carlson & Passerotti, 2010). Four candidate growth models (original von Bertalanffy, typical von Bertalanffy, Gompertz and Richards) were employed to fit length-at-age data obtained from three known-age bottlenose dolphin populations in Bunbury, Shark Bay and Mandurah, Western Australia. Each of the candidate functions applied in the current study have been

widely used to profile the growth of Osteichthyan (Lessa *et al*., 2016) and Chondrichthyan (Cailliet *et al*., 2006; Piercy *et al*., 2010) fishes, as well as cetacean species (McFee *et al*., 2010; Fearnbach *et al*., 2011).

Of the four growth models fitted to length-at-age data derived from laser photogrammetry and historical demographic data respectively, the Richards growth function (RGF) provided the best fit for all sampled populations. For Bunbury and Mandurah, the RGF was the most parsimonious model, with both populations assigned the highest-possible Akaike Information Criterion weighting (AIC*w*) value of one. However, when describing the length-at-age data obtained from Shark Bay, a greater balance became evident between the candidate models. For example, the RGF, original von Bertalanffy (OvB) and typical von Bertalanffy (TvB) models all received strong support, with the RGF ultimately being selected due to its superior AIC*w* score. While the performance of the growth models were comparable for Shark Bay, the large variation in model performance experienced with the Bunbury and Mandurah populations was unexpected.

A possible explanation for this variation may relate to a common dilemma experienced when modelling the early growth of cetacean species - potentially influencing both how well the length-at-age data can be described, and how useful the output parameters are for biological inference. This potential dilemma involves the presence of accelerated postnatal growth experienced by neonatal calves, and the ability of growth models to fit this growth. This issue will now be discussed in relation to the current study, and recommendations provided for future studies.

Marine mammals such as cetaceans generally follow a determinate growth strategy, meaning growth eventually ceases at the attainment of maturity (Mumby *et al*., 2015). Accelerated growth, however, has been observed during the 'critical early period', with growth rates peaking within the first year or two of life, before slowing down abruptly

(McFee *et al*., 2012). This near-exponential growth has been documented in several toothed (odontocete) whale species including the common bottlenose dolphin (*Tursiops truncatus*; Read *et al*., 1993; Mattson *et al*., 2006; McFee *et al*., 2010), Pacific white-sided dolphin (*Lagenorhynchus obliquidens*; Ferrero & Walker, 1996), and finless porpoise (*Neophocaena phocaenoides*; Jefferson *et al*., 2012), as well as in baleen whale (mysticete) species such as the Northern Atlantic right whale (*Eubalaena glacialis*; Fortune *et al*., 2012). One of the drawbacks often associated with continuous growth models, such as the von Bertalanffy growth function (von Bertalanffy, 1938, Beverton & Holt, 1959), is the inability to model this early and rapid growth (Gamito, 1998; Cailliet *et al*., 2006). More specifically, continuous growth models rely on near-linear growth which remains relatively uniform as individuals approach maturity, and therefore struggle to account for those marked fluctuations in growth rates usually observed in early life (Essington, 2001; Fortune *et al*., 2012; Vincenzi *et al*., 2016). When applying this to the current study, fitting the TvB, OvB and GOM models to early postnatal growth proved problematic with the Bunbury and Mandurah populations. This is because the first-year calves experienced accelerated neonatal growth, which subsequently slowed down considerably during the latter stages of their first year. However, this trend was not observed when the RGF was fitted to the length-at-age data of all populations.

Despite being mathematically-equivalent to the TvB, the RGF best described the growth of young individual dolphins sampled in Bunbury and Mandurah. The point of difference between the two models was the application of the shape parameter '*p*' within the RGF equation. This shape parameter has no clear biological interpretation (Ratkowsky, 1983), but enables the inflection point of the curve to be set anywhere between the range of minimum and maximum asymptote values, providing additional flexibility throughout early regions of the curve (i.e. with younger individuals; Birch, 1999; Fearnbach *et al*., 2011). The importance of this flexibility cannot be understated, because it allows researchers to investigate the

natural variability of biological growth among individuals of the same age, while also accounting for environmental influences (Yuancai *et al*., 1997). Ultimately, the flexibility observed in the RGF can accommodate the rapid early growth rates of dolphins in Bunbury and Mandurah. In contrast, no distinct, accelerated growth was detected for young individual dolphins in Shark Bay, possibly due to either an inherent lack of accelerated growth or a lack of data points sampled within the critical early period. This could potentially explain the improved performance of all candidate growth models when fitting Shark Bay dolphin's length-at-age data.

4.4.2 Model convergence of Richards growth function parameters

While the RGF was deemed the most parsimonious of all candidate models, it had difficulty converging (or producing) parameter estimates for each of the sampled populations, which ultimately affected the interpretation of some findings of the study. In essence, growth models apply an iterative algorithm aiming to converge to (or locate) a series of model-specific parameters, which maximise the likelihood that the observed data is represented (Mirmam, 2014). Ultimately, this promotes the notion that model convergence is reliant on the balance between the respective model parameters and the observed length-at-age data. For example, datasets that are either small (restricted age and size range) or variable in nature result in reasonable models failing to converge on parameter estimates (Mirmam, 2014). This was probably the case in the current study, as convergence of asymptotic length (L_∞) estimates were highly dependent on whether the growth model was fitted to sex-specific (male or female) or combined-sex data (pooled male, female and unknown-sex points; **Table 3.3**).

In addition, the complexity of a growth model (i.e. number of parameters) can also influence its ability to yield meaningful parameters. For example, the most complex model in the current set of candidate models is the four-parameter RGF, while the remaining models only

have three. This could potentially result in 'over-parameterisation', i.e. the quality of data required to estimate realistic model parameters does not match the quality of the observed length-at-age data (Paine *et al*., 2012; Bartareau *et al*., 2013).

Given the difficulties experienced in model convergence described above, the combined-sex output parameters derived from the RGF were subsequently deemed unreliable for biological inference. Instead, the selected RGF model was solely used to predict length-at-age, without interpreting parameters of biological significance (e.g. asymptotic length or length-at-birth). For example, the respective predicted length-at-age values, rather than model parameter estimates, were employed to characterise and compare the growth of all three sampled dolphin populations.

In the current study, fitting the rapid, early growth observed in dolphins off Bunbury and Mandurah would not have been possible without the application of the flexible RGF. However, the combined-sex (pooled male, female, and unknown-sex) model parameters derived from this RGF either failed to converge or were difficult to interpret biologically, thus prompting the need for an alternative approach. As such, it is recommended that a biphasic growth model be considered when growth in small odontocete species is investigated.

Biphasic models aim to fit length-at-age data during two distinct growth phases. The first phase represents the critical growth period of young calves, while the second phase accounts for both juvenile and adult individuals displaying marked decreases in growth rate (Fortune *et al*., 2012). Biphasic models, such as the Laird 2-phase model (Jefferson *et al*., 2012), have been endorsed for their ability to characterise multiple growth phases in small odontocete species, such as the common bottlenose dolphin (Cheal & Gales, 1992; McFee *et al*., 2010; McFee *et al*., 2012) and short-beaked common dolphin (*Delphinus delphis*; Danil & Chivers, 2007). Due to the time constraints of this Honours project, the application of biphasic models was outside the scope. It is, however, recommended that future cetacean growth studies

employ biphasic models either as a replacement for continuous models, or that they are, at the very least, used in a complementary manner.

4.4.3 The estimation of biological parameters from selected growth models

Species growth is often described with more than one growth model, as a single model can limit both the quality and quantity of output data available for meaningful inference (Cailliet *et al*., 2006). These limitations are based on the growth model performance, and model selection can be affected by the quality and nature of observed length-at-age data, sample size, as well as the data coverage across age-classes (Prince *et al*., 1991). These factors create uncertainty, which thus emphasises the need to fit multiple growth functions to a species to strengthen the validity of growth descriptions.

In a review of 28 Chondrichthyan growth studies, Cailliet *et al*. (2006) recommended that biologists consider the ability of a model to produce biologically meaningful parameters, in addition to the quality of fit. This allows for the selection of either one or more appropriate growth models using a combination of factors, such as quality of fit and the potential for biological interpretation. This was the case in the current study, in which the RGF curves best described each population's growth but failed to provide biologically meaningful model parameters for the Mandurah and Bunbury populations. As a result, asymptotic length (L_∞) and length-at-birth (L_0) estimates were derived from the OvB growth model and were examined to investigate the growth characteristics of each population further.

Based on the laser-derived measurements obtained on very young dolphin individuals in each of the populations, the OvB model determined that several length-at-birth parameter estimates were biologically robust. For example, all sampled dolphin calves that were deemed less than two weeks old (N= 5) returned BH-DF measurements that were between 32.44 and 35.83 cm. A very young but seemingly healthy dolphin was euthanised, and its

post-mortem provided supporting evidence of a BH-DF measurement of 33.30 cm, thus validating the OvB model results.

For curves of male, female and unknown-sex individuals, OvB results overestimated length-at-birth values for Bunbury neonates, most likely related to the accelerated growth during the critical early period (Neuenhoff *et al*., 2011). However, when focusing on unknown-sex individuals in Mandurah in isolation (*N*=6), relatively tight length-at-birth estimates ranged between 33.07 and 35.54 cm. While it was not possible to determine the sex of these six neonatal individuals, the age estimates were of high quality (i.e. accurate to less than two weeks), instilling confidence in the corresponding length-at-birth estimates. Overall, L_0 estimates for Shark Bay dolphins were comparable to those of Mandurah and ranged between 28.7 and 35.50 cm, thereby suggesting a similar if not slightly smaller size at birth. However, as only one neonatal calf was sampled, these estimates must be interpreted with caution. Regardless, they represented the first BH-DF length estimates of newborn coastal bottlenose dolphin populations from Bunbury, Shark Bay and Mandurah.

The combined-sex RGF curves for Bunbury and Mandurah both failed to reach a clear asymptote, based on either a lack of or overestimation of L_∞ values. Rather, growth continued as Bunbury individuals approached maximum age. For example, the age required to reach the overestimated asymptotic length (mean L_∞= 85.32 cm) exceeded the known lifespan of an Indo-Pacific bottlenose dolphin (~45 years; Cockcroft & Ross, 1990). This is most likely the result of how the growth curve was weighted, as most sampled individuals fell into age classes younger than 25 years and with an inadequate number of individuals older than 25 years to level the asymptote. The lack of an asymptote could also have reflected the variable growth rates in adult dolphins resulting from fluctuations in prey availability (Fearnbach *et al*., 2011) or the presence of somatic growth throughout lifespans.

The L_∞ estimates derived from the alternative OvB model, however, proved to be biologically reasonable for all populations. The estimates for Bunbury and Mandurah were similar to the BH-DF lengths obtained from mature post-mortem subjects (mean L_∞= 78.35 cm & 77.75 cm, respectively; **Table 3.1**) This provided useful preliminary L_∞ estimates that may be investigated in greater depth in subsequent studies. A combination of comprehensive age-class representation and tight growth model fits for the Shark Bay population resulted in a dependable mean L_∞ estimate of 63.34 cm.

The length-at-birth and asymptotic length parameter values reported in the current study cannot be compared with those of other coastal bottlenose dolphin populations, as no growth studies on coastal bottlenose dolphins have employed BH-DF length as a dedicated morphometric measurement. Despite this, these parameter values provide a reference point for future research and monitoring effort, where laser photogrammetry can be used to sample new coastal bottlenose dolphin populations. Moreover, if the current BH-DF measurement can be converted into TBL estimates, it may be possible to conduct retrospective analyses where growth parameter estimates can be compared.

Future studies utilise the morphometric and demographic data available for Bunbury and Shark Bay to further investigate the relationships between length and age at various life history stages. For example, length-at-age estimates of individuals at birth, weaning, sexual maturity and first reproduction would be beneficial for population comparison (Bartareau *et al*., 2013). By comparing these parameters across coastal bottlenose dolphin populations, researchers can elucidate specific adaptations to local habitats and population structures, thereby providing insight into how these populations would respond to fluctuating ecological factors and anthropogenic threats (Chivers *et al*., 2016; Fearnbach *et al*., 2011).

Traditionally, cetacean growth studies aiming to obtain growth parameters have relied on stranding and by-catch specimens which provide data on multiple individuals in a particular snap shot of time (cross-sectional data). Alternatively, longitudinal data has been collected by repeatedly measuring the same live individuals over time, providing increased statistical power due to the reduced influence of bias (McFee *et al*., 2010). However, only captive and capture-release programs could provide opportunities to collect such data, prior to the emergence of photogrammetry. The current study demonstrated the value of non-invasive laser photogrammetry as a morphometric technique, as it was possible to efficiently obtain biologically meaningful parameter estimates on free-ranging dolphins, with the added potential of collecting longitudinal morphometric data in subsequent studies.

4.5 Investigating morphological differences between populations

In the current study, fitting growth curves to laser-derived, length-at-age data provided a unique opportunity to compare growth between two, geographically-isolated populations of coastal bottlenose dolphins (i.e. Bunbury and Shark Bay). To date, laser photogrammetry was never employed specifically to establish and quantify morphological differences between cetacean populations. The findings of this study demonstrated the value of this non-invasive technique to identify and describe morphotypic forms of bottlenose dolphins.

While a few qualitative accounts briefly described some superficial differences in body size between the dolphins residing in Bunbury and Shark Bay (Mann *et al*., 2000; Manlik *et al*., 2016), no empirical evidence was presented to date. In the current study, traditional growth model parameters (such as L_∞ and L_0) were not applied directly to compare populations. Despite this, significant ($p < 0.001$) differences in BH-DF length-at-age (years 1, 3, 12, and 25) were detected between dolphins in Bunbury and Shark Bay.

In most cases, geographical variations in external morphology are influenced by a complex interplay between both environmental and genetic plasticity (Secchi *et al*., 2003). As such,

the observed differences in BH-DF length between Bunbury and Shark Bay individuals may reflect either environmental (phenotypic) or genetic (genotypic) factors, which can only be answered adequately by subsequent studies that utilise and apply a combination of appropriate morphometric and molecular data. In the meantime, the following discussion presents possible explanations for the clear geographical differences in external morphology (body size-at-age) that were identified using non-invasive laser photogrammetry.

Inter- and intra-specific differences in external morphology of odontocete species were documented for short-beaked common dolphins (Murphy & Rogan, 2006), harbour porpoises (*Phocoena phocoena;* Galatius & Gol'din, 2011), Risso's dolphins (*Grampus griseus*; Chen *et al*., 2011), and bottlenose dolphins (Morteo *et al.*, 2017). Given their wide geographical distribution, bottlenose dolphins occupy a diverse range of ecological habitats and consequently demonstrate substantial inter-specific phenotypic variation (Mendez *et al*., 2013). Morphometric investigations into these phenotypic variations documented latitudinal gradients in body size, with bottlenose dolphins originating from warmer waters significantly shorter in total length compared to those living in cooler, temperate waters (Ross & Cockcroft, 1990; Gao *et al*., 1995; McFee *et al*., 2012). Consequently, ambient temperature is regarded as a dominant factor in the formation of latitudinal clines in body size.

The inverse relationship between sea surface temperature and body size is characteristic of the well-known ecogeographic rule (i.e. Bergmann's rule), in which the anatomist Carl Bergmann postulated the following: the body length of closely-related, vertebrate species in cooler regions tend to exhibit greater lengths than those residing in warmer waters (Bergmann, 1847). This pattern is the result of a temperature budget mechanism which defines and describes a trade-off between surface area and volume, where the surface area of an endothermic animal represents its ability to dissipate heat, while its volume serves as

a measure of its heat generation capability (Salewski & Watt, 2017). A reduced surface-to-volume ratio is thus considered a selective advantage, which enables large-bodied animals residing in cold environments to retain body heat more effectively (Blackburn *et al*., 1999; Torres-Romero *et al*., 2016).

The Bunbury and Shark Bay study sites are located approximately 1,000 km apart, equating to a latitudinal difference of approximately eight degrees. Given its Mediterranean climate of hot, dry summers and relatively wet winters, the atmospheric and oceanographic conditions within Bunbury are susceptible to distinct seasonal fluctuations (McCluskey *et al*., 2016). In Bunbury, during the austral summer months (i.e. December to February), coastal sea surface temperature (SST) peaks at 23°C, with a minimum SST of 14°C occurring during the winter months between June and August (Smith, 2012). In contrast, the climate of Shark Bay is considered subtropical (Kopps *et al*., 2013), characterised by prolonged warmer periods with relatively shorter, milder winters. For example, the months between September and May are the hottest, with SSTs constantly exceeding 23°C (maximum =27°C, while the cooler months between June and August can exhibit minimum SSTs of 14°C (Heithaus & Dill, 2002).

Assuming the Lo estimates for Bunbury (33.30 cm) and Shark Bay (32.02 cm) were biologically robust, the intra-specific differences in early growth strategy were pronounced. For example, using the RGF model, Bunbury calves were estimated to grow to a mean BH-DF length of 50.43 cm by the end of their first year, suggesting an increase in BH-DF length of at least 17 cm. The Shark Bay conspecifics yielded a significantly lower BH-DF length estimate of 38.28 cm (**Table 3.3**), indicating an increase of only 6 cm during the first year. These contrasting growth strategies could result from differences in timing of their calving seasons, as Bunbury calves are born typically during the early autumn months of March and April (Smith *et al*., 2016), while the Shark Bay calving season peaks between October and December (Mann *et*

al., 2000). As a result, neonatal calves in Bunbury have a shorter period to prepare for the colder, winter months between June and September. Newborn calves in Shark Bay, on the other hand, are usually born at the beginning or in the middle of summer, when water temperatures are at their highest. This allows far greater time to develop physically before the onset of winter.

For mother dolphins, the cost of lactation and growth is undoubtedly high (Malinowski & Herzing, 2015). In essence, the postnatal development of calves is, in part, dependent on the quality and quantity of prey available to the lactating mother. In Bunbury, McCluskey *et al*. (2016) reported that while a higher abundance of prey was present during summer, prey items of greater size and calorific value were captured during the cooler, winter months. In spite of the reduced supply of prey in winter, it may be reasonable to suggest it is the high calorific value of these prey items which could be sustaining lactating mothers, and causing the accelerated growth of young calves residing in the coastal and estuarine waters of Bunbury (McCluskey *et al*., 2016; Smith *et al*., 2016). In Shark Bay, however, no distinct seasonal fluctuations in prey availability have been identified (Heithaus & Dill, 2002).

The ability to differentiate between distinct species or intra-specific populations, as well as the in-depth knowledge of the contributing drivers of divergence, enable researchers to identify biologically meaningful conservation units. Evidence of divergence and a strong population structure in coastal bottlenose dolphins can influence the way managers formulate and implement conservation strategies, given those populations that do not reproductively exchange may be at greater risk of local extinction.

Most early cetacean studies investigating regional variations in morphology relied solely on measurement data obtained from either post-mortem subjects or by using highly-invasive, capture-release techniques. For example, subtle variations found in skull and spine morphology (i.e. size and shape) have been extensively used to discriminate between intra-

specific populations of short-beaked common dolphins (Murphy & Rogan, 2006; Pinela *et al*., 2011), harbour porpoises (Gol'din & Vishnyakova, 2016) common bottlenose dolphins (Costa *et al*., 2016) and Franciscana dolphins (*Pontoporia blainvillei*; Higa *et al*., 2002). These detailed morphometric investigations would not have been possible without the use of post-mortem subjects sourced through stranding events and fisheries by-catch.

While a large number of cetacean studies have benefited from the use of post-mortem subjects by obtaining valuable morphometric data, some of the associated limitations of this method warrants mentioning. For instance, the lack of sampling structure associated with post-mortem events can cause an over- or under-representation of groups, resulting in potential sampling bias. Accordingly, using emaciated or diseased dolphin individuals in research may not be representative of the population from which they originated (Peltier *et al*., 2012), and the degree to which this could influence skeletal measurements is unknown. Thus, biologists must be aware of potential sources of sampling bias when making biological inferences using post-mortem subjects.

The use of live, temporarily captured dolphin subjects may significantly improve the level of representativeness achieved than is the case with post-mortem subjects, because physical measurements can be obtained from pre-selected individuals (Fair *et al*., 2006; Wells *et al*., 2009). However, ethical obligations place restrictions on which age classes can be physically captured, and this negatively impacts on the wider applicability of this data collection technique. For example, McFee *et al*. (2012) utilised health assessment capture-release programs in Florida and South Carolina, United States of America, to investigate patterns of growth between the two geographically separated bottlenose dolphin populations. While the physical captures made accurate morphometric measurements and tooth extractions for age estimation possible, the permit restrictions placed on the capture of mother and calf pairs (where the calf was under the age of two years) precluded investigation into their early

growth. As a result, McFee *et al*. (2012) were not able to document or compare the population-specific critical early periods, during which growth rates are considered to be greatest (Read *et al*., 1993; Ferrero & Walker, 1996; Mattson *et al*., 2006).

The combination of morphometric and genetic analyses allows for complementary investigations into the ecological, genetic and evolutionary factors influencing intra-specific divergence (Mendez *et al*., 2013). However, by using laser photogrammetry, morphometric data can now be obtained in a more efficient manner. Not only can researchers increase their sample sizes in a relatively short time period, but they can also obtain morphometric data that is more representative of the free-ranging population being sampled.

5. Conclusion

The primary objective of this study was to investigate the feasibility and precision of laser photogrammetry, as a means to obtain morphometric data on free-ranging coastal bottlenose dolphins.

The secondary objectives of the study aimed to demonstrate the value of laser photogrammetry by providing empirical examples of how this non-invasive technique can be applied on free-ranging dolphins, including:

1. Developing length-at-age growth curves using dolphin populations of known-age
2. Investigating morphological differences between populations

Potential sources of error relating to laser photogrammetry were quantified using two- and three-dimensional experiments, as well as opportunistic post-mortem subjects. When horizontal angles were minimised (< 15°), photographs provided reliable BH-DF length measurements. Coefficient of variation (CV) values obtained from Bunbury, Shark Bay and Mandurah measurements compared favourably to those CV values reported in similar

photogrammetric studies (< 2 %), providing confidence in the precision of laser photogrammetry.

The feasibility of laser photogrammetry as a morphometric technique is clear, with its accuracy, mobility and non-invasive approach considered highly advantageous when compared to traditional morphometric techniques. As such, population growth curves were successfully developed using known-age individuals from each of the study populations, providing invaluable opportunities to investigate population-specific growth using length-at-age data and growth parameters (length at birth and asymptotic length). These growth estimates should prove most useful for similar growth studies in the future by providing reference values for group comparison.

The population growth curves developed facilitated the establishment of detailed length-at-age growth comparisons between Bunbury and Shark Bay. Length-at-age estimates for Bunbury individuals were significantly longer than for their Shark Bay counterparts, providing compelling evidence in favour of the existence of morphotypic variation between intra-specific populations of coastal bottlenose dolphins. When used in combination with molecular analyses, morphometric data of this nature should provide the basis for future studies that investigate biological, ecological and genetic factors influencing intra-specific variations in growth.

6. References

Akaike, H. (1974). A new look at the statistical model identification. *IEEE Transactions on Automatic Control, 19*(6), 716 – 723. doi: 10.1109/TAC.1974.1100705.

Auttila, M., Kurkilahti, M., Niemi, M., Levänen, R., Sipilä, T., Isomursu, M., & Kunnasranta, M. (2016). Morphometrics, body condition, and growth of the ringed seal (*Pusa hispida saimensis*) in Lake Saimaa: Implications for conservation. *Marine Mammal Science, 32*(1), 252-267. doi: 10.1111/mms.12256.

Baker, A. N., Smith, A. N. H., & Pichler, F. B. (2002). Geographical variation in Hector's dolphin: Recognition of new subspecies of *Cephalorhynchus hectori*. *Journal of the Royal Society of New Zealand, 32*(4), 713-727. doi: 10.1080/03014223.2002.9517717.

Bartareau, T., Onorato, D., & Jansen, D. (2013). Growth in body length and mass of the Florida panther: an evaluation of different models and sexual size dimorphism. *Southeastern Naturalist, 12*, 27-40.

Bergeron, P. (2007). Parallel lasers for remote measurements of morphological traits. *Journal of Wildlife Management, 71*(1), 289-292. doi: 10.2193/2006-290

Bergmann, Carl (1847). "Über die Verhältnisse der Wärmeökonomie der Thiere zu ihrer Grösse". Göttinger Studien. 3, 595-708.

Best, P. B., & Rüther, H. (1992). Aerial photogrammetry of southern right whales, *Eubalaena australis*. *Journal of Zoology, 228*(4), 595-614. doi: 10.1111/j.1469-7998.1992.tb04458.x.

Bester, L., & de Bruyn, P. J. N. (2015). Simplifying photogrammetric analysis for assessment of large mammal mass: automated targeting and 3D model building. *The Photogrammetric Record, 30*(150), 227-241. doi: 10.1111/phor.12102.

Beverton, R.J.H., & Holt, S.J. (1959) A review of the lifespan and mortality rates of fish in nature and their relationship to growth and other physiological characteristics. *Ciba Foundation Colloquim on Ageing*, *5,* 142-160.

Birch, C.P.D. (1999). A new generalized logistic sigmoid growth equation compared with the Richards growth equation. *Annals of Botany, 83*, 713-723.

Blackburn, T.M., Lawton, J.H., & Gaston, K.J. (1998). Patterns in the geographic ranges of the world's woodpeckers. *Ibis, 140*(4), 626-638. doi: 10.1111/j.1474-919X.1998.

Blackwell, G. L., Bassett, S. M., & Dickman, C. R. (2006). Measurement error associated with external measurements commonly used in small-mammal studies. *Journal of Mammalogy, 87*(2), 216-223. doi: 10.1644/05-mamm-a-215r1.1.

Blomquist, G. E., Kowalewski, M. M., & Leigh, S. R. (2009). Demographic and morphological perspectives on life history evolution and conservation of new world monkeys. In: P. A. Garber, A. Estrada, J. C. Bicca-Marques, E. W. Heymann, & K. B. Strier (Eds.), *South American Primates: Comparative Perspectives in the Study of Behavior, Ecology, and Conservation* (117-138). New York, NY: Springer New York.

Bräger, S., & Chong, A. K. (1999). An application of close range photogrammetry in dolphin studies. *The Photogrammetric Record, 16*(93), 503-517. doi: 10.1111/0031-868x.00139.

Brown, A. M., Bejder, L., Parra, G. J., Cagnazzi, D., Hunt, T., Smith, J. L., & Allen, S. J. (2016). Chapter Ten - Sexual dimorphism and geographic variation in dorsal fin features of Australian humpback dolphins, *Sousa sahulensis*. In A. J. Thomas & E. C. Barbara (Eds.), *Advances in Marine Biology* (pp. 273-314): Academic Press.

Burnham, K.P., & Anderson, D.R. (2002). Model selection and multimodel inference: a practical information-theoretic approach. New York, USA: Springer.

Cailliet, G. M., Smith, W. D., Mollet, H. F., & Goldman, K. J. (2006). Age and growth studies of chondrichthyan fishes: the need for consistency in terminology, verification, validation, and growth function fitting. *Environmental Biology of Fishes, 77*(3), 211-228. doi: 10.1007/s10641-006-9105-5.

Campana, S. E. (2001). Accuracy, precision and quality control in age determination, including a review of the use and abuse of age validation methods. *Journal of Fish Biology, 59*(2), 197-242. doi: 10.1111/j.1095-8649.2001.tb00127.x

Caswell, H. (2012). Matrix models and sensitivity analysis of populations classified by age and stage: a vec-permutation matrix approach. *Theoretical Ecology, 5*(3), 403-417. doi: 10.1007/s12080-011-0132-2

Charlton-Robb, K., Gershwin, L., Thompson, R., Austin, J., Owen, K., & McKechnie, S. (2011). A New Dolphin Species, the Burrunan Dolphin *Tursiops australis* sp. nov., Endemic to Southern Australian Coastal Waters. *PLoS ONE, 6*. doi: 10.1371/journal.pone.002404.

Cheal, A. J., & Gales, N. J. (1991). Body mass and food intake in captive, breeding bottlenose dolphins, *Tursiops truncatus*. *Zoo Biology, 10*(6), 451-456. doi: 10.1002/zoo.1430100603.

Chen, I., Watson, A., & Chou, L. S. (2011). Insights from life history traits of Risso's dolphins (*Grampus griseus*) in Taiwanese waters: shorter body length characterizes northwest Pacific population. *Marine Mammal Science, 27*(2), 43-64. doi: 10.1111/j.1748-7692.2010.00429.x.

Cheney, B., Wells, R.S., & Thompson, P.M. (2015). *Investigating individual growth rates in wild bottlenose dolphins using remote laser photogrammetry*. Poster presented at the SMM Biennial Conference on the Biology of Marine Mammals, San Francisco, CA. 13-18 December, 2015.

Chivers, S. J., Perryman, W. L., Lynn, M. S., Gerrodette, T., Archer, F. I., Danil, K., & Dines, J. P. (2016). Comparison of reproductive parameters for populations of eastern North Pacific common dolphins: *Delphinus capensis* and *D. delphis*. *Marine Mammal Science, 32*. doi: 10.1111/mms.12244.

Christiansen, F., Dujon, A. M., Sprogis, K. R., Arnould, J. P. Y., & Bejder, L. (2016). Non-invasive unmanned aerial vehicle provides estimates of the energetic cost of reproduction in humpback whales. *Ecosphere, 7*(10). doi: 10.1002/ecs2.1468.

Clapham, P. J. (1992). Age at attainment of sexual maturity in humpback whales, *Megaptera novaeangliae*. *Canadian Journal of Zoology, 70*(7), 1470-1472. doi: 10.1139/z92-202.

Clark, S. T., & Odell, D. K. (1999). Allometric relationships and sexual dimorphism in captive killer whales (*Orcinus orca*). *Journal of Mammalogy, 80*(3), 777-785.

Cockcroft, V. G., & Ross, G. J. B. (1990). Age, growth, and reproduction of bottlenose dolphins, *Tursiops truncatus*, from the east coast of South Africa. *Fishery Bulletin*, *88, 289-302*.

Connor, R. C., & Krutzen, M. (2015). Male dolphin alliances in Shark Bay: changing perspectives in a 30-year study. *Animal behaviour, 103*, 223-235. doi: 10.1016/j.anbehav.2015.02.019.

Costa, A. P. B., Rosel, P. E., Daura-Jorge, F. G., & Simões-Lopes, P. C. (2016). Offshore and coastal common bottlenose dolphins of the western South Atlantic face-to-face: What the skull and the spine can tell us. *Marine Mammal Science, 32*(4), 1433-1457. doi: 10.1111/mms.12342.

Cranford, T. W. (1999). The Sperm Whale's nose: sexual selection on a grand scale? *Marine Mammal Science, 15*(4), 1133-1157. doi: 10.1111/j.1748-7692.1999.tb00882.x.

Cunha, H. A., Medeiros, B. V., Barbosa, L. A., Cremer, M. J., Marigo, J., Lailson-Brito, J., & Solé-Cava, A. M. (2014). Population Structure of the Endangered Franciscana Dolphin (*Pontoporia blainvillei*): Reassessing Management Units. *PLoS ONE, 9*(1), e85633. doi: 10.1371/journal.pone.0085633.

Danil, K., & Chivers, S.J. (2007). Growth and reproduction of female short-beaked common dolphins, *Delphinus delphis*, in the eastern tropical Pacific. *Canadian Journal of Zoology*, *85*(1), 108-121,. doi: 10.1139/z06-188.

Dawson, S.M., Chessudm, C.J., Hunt, P.J., Slooten, E. (1995). An inexpensive, stereophotographic technique to measure sperm whales from small boats. Report of the International Whaling Commission, 431-436.

Deakos, M. H. (2012). The reproductive ecology of resident manta rays (*Manta alfredi*) off Maui, Hawaii, with an emphasis on body size. *Environmental Biology of Fishes, 94*(2), 443-456. doi: 10.1007/s10641-011-9953-5.

del Castillo, D. L., Flores, D. A., & Cappozzo, H. L. (2014). Ontogenetic development and sexual dimorphism of franciscana dolphin skull: A 3D geometric morphometric approach. *Journal of Morphology, 275*(12), 1366-1375. doi: 10.1002/jmor.20309.

Dellabianca, N. A., Hohn, A. A., Goodall, R. N. P., Pousa, J. L., MacLeod, C. D., & Lima, M. (2012). Influence of climate oscillations on dentinal deposition in teeth of Commerson's dolphin. *Global Change Biology, 18*(8), 2477-2486. doi: 10.1111/j.1365-2486.2012.02707.x.

Development Core Team (2013). R: A language and environment for statistical computing. R Foundation for Statistical Computing, Vienna, Austria. ISBN 3-900051-07-0, URL link: http://www.R-project.org/.

Durban, J. W., & Parsons, K. M. (2006). Laser-metrics of free-ranging killer whales. *Marine Mammal Science, 22*(3), 735-743. doi: 10.1111/j.1748-7692.2006.00068.x.

Enberg, K., Dunlop, E. S., & Jørgensen, C. (2008). Fish growth. In: Jørgensen S.E., & Fath, B.D. (eds), Encyclopedia of ecology (1564-1572). Oxford, UK: Elsevier.

English, S., Bateman, A. W., & Clutton-Brock, T. H. (2012). Lifetime growth in wild meerkats: incorporating life history and environmental factors into a standard growth model. *Oecologia, 169*(1), 143+.

Epperly, S. P., Braun, J., Chester, A. J., Cross, F. A., Merriner, J. V., Tester, P. A., & Churchill, J. H. (1996). Beach strandings as an indicator of at-sea mortality of sea turtles. *Bulletin of Marine Science, 59*(2), 289-297.

Essington, T.E., Kitchell, J.F., & Walters, C.J. (2001). The Von Bertalanffy growth function, bioenergetics, and the consumption rates of fish. *Canadian Journal of Fisheries and Aquatic Sciences, 58*(11), 2129-2138. doi: 10.1139/cjfas-58-11-2129.

Evans, K., Hindell, M. A., & Thiele, D. (2003). Body fat and condition in sperm whales, *Physeter macrocephalus*, from southern Australian waters. *Comparative Biochemistry and Physiology Part A: Molecular & Integrative Physiology, 134*(4), 847-862. doi: http://dx.doi.org/10.1016/S1095-6433(03)00045-X.

Fair, P. A., Adams, J. D., Zolman, E., McCulloch, S. D., Goldstein, J. D., Murdoch, M. E., & Bossart, G. D. (2006). *Protocols for conducting dolphin capture-release health assessment studies* (NOAA Technical Memorandum NOS NCCOS 49). Silver Spring, MD: National Oceanic and Atmospheric Administration. p 83.

Fearnbach, H., Durban, J.W., Ellifrit, D.K., & Balcomb, K.C. (2011). Size and long-term growth trends of endangered fish-eating killer whales. *Endangered Species Research*, *13*, 173-180.

Ferrero, R. C., & Walker, W. A. (1996). Age, growth, and reproductive patterns of the Pacific white-sided dolphin (*Lagenorhynchus obliquidens*) taken in high seas drift nets in the central North Pacific Ocean. *Canadian Journal of Zoology, 74*(9), 1673-1687. doi: 10.1139/z96-185.

Ford, J. K. B., Ellis, G. M., Olesiuk, P. F., & Balcomb, K. C. (2010). Linking killer whale survival and prey abundance: food limitation in the oceans' apex predator? *Biology Letters, 6*(1), 139-42. doi: 10.1098/rsbl.2009.0468.

Fortune, S. M. E., Trites, A. W., Perryman, W. L., Moore, M. J., Pettis, H. M., & Lynn, M. S. (2012). Growth and rapid early development of North Atlantic right whales (*Eubalaena glacialis*). *Journal of Mammalogy, 93*(5), 1342-1354.
. doi: 10.1644/11-mamm-a-297.1.

Frainer, G., Huggenberger, S., & Moreno, I. B. (2015). Postnatal development of franciscana's (*Pontoporia blainvillei*) biosonar relevant structures with potential implications for function, life history, and bycatch. *Marine Mammal Science, 31*(3), 1193-1212. doi: 10.1111/mms.12211.

Gabriele, C. M., Lockyer, C., Straley, J. M., Jurasz, C. M., & Kato, H. (2010). Sighting history of a naturally marked humpback whale (*Megaptera novaeangliae*) suggests ear plug growth layer groups are deposited annually. *Marine Mammal Science, 26*(2), 443-450. doi: 10.1111/j.1748-7692.2009.00341.x.

Galatius, A., Berta, A., Frandsen, M. S., & Goodall, R. N. P. (2011). Interspecific variation of ontogeny and skull shape among porpoises (*Phocoenidae*). *Journal of Morphology, 272*(2), 136-148. doi: 10.1002/jmor.10900.

Galbany, J., Stoinski, T. S., Abavandimwe, D., Breuer, T., Rutkowski, W., Batista, N. V., & McFarlin, S. C. (2016). Validation of two independent photogrammetric techniques for determining body measurements of gorillas. *American Journal of Primatology, 78*(4)*,* 418-431. doi: 10.1002/ajp.22511.

Gamito, S. (1998). Growth models and their use in ecological modelling: an application to a fish population. *Ecological Modelling, 113*(1), 83-94. doi.org/10.1016/S0304-3800.

Gao, A., Zhou, K., & Wang, Y. (1995). Geographical variation in morphology of bottlenose dolphins (*Tursiops sp.)* in Chinese waters. *Aquatic Mammals, 21*(2), 121-135.

Garde, E., Frie, A. K., Dunshea, G., Hansen, S. H., Kovacs, K. M., & Lydersen, C. (2010). Harp seal ageing technique – teeth, aspartic acid racemization, and telomere sequence analysis. *Journal of Mammalogy, 91*(6), 1365-1374.
doi: https://doi.org/10.1644/10-MAMM-A-080.1.

Garde, E., Heide-Jørgensen, M. P., Ditlevsen, S., & Hansen, S. H. (2012). Aspartic acid racemization rate in narwhal (*Monodon monoceros*) eye lens nuclei estimated by counting of growth layers in tusks. *Polar Research, 31*(1). doi: 10.3402/polar.v31i0.15865.

George, J. C., Bada, J., Zeh, J., Scott, L., & *et al*. (1999). Age and growth estimates of bowhead whales (*Balaena mysticetus*) via aspartic acid racemization. *Canadian Journal of Zoology, 77*(4), 571-580.

Goldin, P.E., & Vishnyakova, K.A. (2015). Differences in skull size of harbour porpoises*, Phocoena phocoena (Cetacea),* in the sea of azov and the black sea: evidence for different morphotypes and populations*. Vestnik zoologi, 49(2), 171-180.* doi: *10.1515/vzoo-2015-0017.*

Gómez-Campos, E., Borrell, A., & Aguilar, A. (2011). Assessment of nutritional condition indices across reproductive states in the striped dolphin (*Stenella coeruleoalba*). *Journal of Experimental Marine Biology and Ecology, 405*(1–2), 18-24. doi: http://dx.doi.org/10.1016/j.jembe.2011.05.013.

Gompertz, B. (1825). On the nature of the function expressive of the law of human mortality, and on a new mode of determining the value of life contingencies. *Philosophical Transactions of the Royal Society of London, 115*, 513-583.

Groeneveld, L. F., Rasoloarison, R. M., & Kappeler, P. M. (2011). Morphometrics confirm taxonomic deflation in dwarf lemurs (Primates: Cheirogaleidae), as suggested by genetics. *Zoological Journal of the Linnean Society, 161*(1), 229-244 doi: 10.1111/j.1096-3642.2010.00634.x.

Growcott, A., Miller, B., Sirguey, P., Slooten, E., & Dawson, S. (2011). Measuring body length of male sperm whales from their clicks: The relationship between inter-pulse intervals and photogrammetrically measured lengths. *Journal of the Acoustical Society of America, 130*(1), 568-573. doi: 10.1121/1.3578455.

Hale, P. T., Barreto, A. S. and Ross, G. J. (2000). Comparative morphology and distribution of the *aduncus* and *truncatus* forms of bottlenose dolphin *Tursiops* in the Indian and Western Pacific Oceans. *Aquatic Mammals*, *26*(2), 101-110.

Hart, L. B., Wells, R. S., & Schwacke, L. H. (2013). Reference ranges for body condition in wild bottlenose dolphins *Tursiops truncatus*. *Aquatic Biology, 18*, 63-68.

Heithaus, M. R., & Dill, L. M. (2002). Food availability and tiger shark predation risk influence bottlenose dolphin habitat use. *Ecology, 83*(2), 480-491. doi: 10.2307/2680029.

Higa, A., Hingst-Zaher, E., & Vivo, M. (2002). Size and shape variability in the skull of *Pontoporia blainvillei* (*Cetacea: Pontoporiidae*) from the Brazilian coast. *Latin American Journal of Aquatic Mammals*, *1*(1), 145-152. doi:10.5597/lajam00018.

Hoekstra, P. F., Wong, C. S., O'Hara, T. M., Solomon, K. R., Mabury, S. A., & Muir, D. C. G. (2002). Enantiomer-specific accumulation of PCB atropisomers in the bowhead whale (*Balaena mysticetus*). *Environmental Science & Technology, 3*6(7), 1419–1425 doi: 10.1021/es015763g.

Hunt, K. E., Stimmelmayr, R., George, C., Hanns, C., Suydam, R., Brower, H., & Rolland, R. M. (2014). Baleen hormones: a novel tool for retrospective assessment of stress and reproduction in bowhead whales (*Balaena mysticetus*). *Conservation Physiology, 2*(1). doi: 10.1093/conphys/cou030.

Irvine, A. B., Scott, M. D., Wells, R. S., & Kaufmann, J. H. (1981). Movements and activities of the Atlantic bottlenose dolphin *Tursiops truncatus*, near Sarasota, Florida (Tampa Bay, Gulf of Mexico). *Fishery Bulletin, 79*(4), 671-688.

Jaquet, N. (2006). A simple photogrammetric technique to measure sperm whales at sea. *Marine Mammal Science, 22*(4), 862-879. doi: 10.1111/j.1748-7692.2006.00060.x.

Jefferson, T.A., Hung, S.K., Robertson, K.M., & Archer, F.I. (2012). Life history of the Indo-Pacific humpback dolphin in the Pearl River Estuary, southern China. *Marine Mammal Science, 28*(1), 84-104. doi: 10.1111/j.1748-7692.2010.00462.x.

Jordan, F. F. J., Murphy, S., Martinez, E., Amiot, C., van Helden, A., & Stockin, K. A. (2015). Criteria for assessing maturity of skulls in the common dolphin, *Delphinus sp*., from New Zealand waters. *Marine Mammal Science, 31*(3), 1077-1097. doi: 10.1111/mms.12229.

Karniski, C., Patterson, E. M., Krzyszczyk, E., Foroughirad, V., Stanton, M. A., & Mann, J. (2015). A comparison of survey and focal follow methods for estimating individual activity budgets of cetaceans. *Marine Mammal Science, 31*(3), 839-852. doi: 10.1111/mms.1219.

Kastelein, R. A., Triesscheijn, R. J. V., & Jennings, N. (2016). Reversible bending of the dorsal fins of harbor porpoises (*Phocoena phocoena*) and a striped dolphin (*Stenella coeruleoalba*) in captivity. *Aquatic Mammals, 42*(2), 218-226. doi: http://dx.doi.org/10.1578/AM.42.2.2016.218.

Katsanevakis, S. (2006). Modelling fish growth: Model selection, multi-model inference and model selection uncertainty. *Fisheries Research, 81*(2–3), 229-235. doi: http://doi.org/10.1016/j.fishres.2006.07.002.

Kemper, C. M., Trentin, E., & Tomo, I. (2014). Sexual maturity in male Indo-Pacific bottlenose dolphins (*Tursiops aduncus*): evidence for regressed/pathological adults. *Journal of Mammalogy, 95*(2), 357-368. doi: 10.1644/13-mamm-a-007.1.

Klimley, A. P., & Brown, S. T. (1983). Stereophotography for the field biologist: measurement of lengths and three-dimensional positions of free-swimming sharks. *Marine Biology, 74*(2), 175-185. doi: 10.1007/bf00413921.

Klütsch, C. F. C., Misof, B., Grosse, W. R., & Moritz, R. F. A. (2007). Genetic and morphometric differentiation among island populations of two Norops lizards (Reptilia: Sauria: Polychrotidae) on independently colonized islands of the Islas de Bahia (Honduras). *Journal of Biogeography, 34*(7), 1124-1135. doi: 10.1111/j.1365-2699.2007.01691.x.

Kopps, A. M., Krützen, M., Allen, S. J., Bacher, K., & Sherwin, W. B. (2014). Characterizing the socially transmitted foraging tactic “sponging” by bottlenose dolphins (*Tursiops sp*.) in the western gulf of Shark Bay, Western Australia. *Marine Mammal Science, 30*(3), 847-863. doi: 10.1111/mms.12089.

Krzyszczyk, E., & Mann, J. (2012). Why become speckled? Ontogeny and function of speckling in Shark Bay bottlenose dolphins (*Tursiops sp*.). *Marine Mammal Science, 28*(2), 295-307. doi: 10.1111/j.1748-7692.2011.00483.x.

Lessa, R., & Santana, F. M. (2016). Growth of the dolphinfish *Coryphaena hippurus* from north-eastern Brazil with an appraisal of the efficacy of scales and otoliths for ageing. *Journal of Fish Biology, 89*(1), 977-989. doi: 10.1111/jfb.13002.

Leurs, G., O'Connell, C. P., Andreotti, S., Rutzen, M., & Vonk Noordegraaf, H. (2015). Risks and advantages of using surface laser photogrammetry on free-ranging marine organisms: a case study on white sharks *Carcharodon carcharias*. *Journal of Fish Biology, 86*(6), 1713-1728. doi: 10.1111/jfb.12678.

Lockyer, C. (1984*)*. Review of baleen whale (Mysticeti) reproduction and implications for management. Report of the International Whaling Commission, 627– 650.

Lockyer, C., Hohn, A. A., Doidge, D. W., Heide-Jørgensen, M. P., & Suydam, R. (2007). Age determination in belugas (*Delphinapterus leucas*): A quest for validation of dentinal layering. *Aquatic Mammals, 33*(3), 293-304.

Lubetkin, S. C. (2008). *Using annual cycles of stable carbon isotope ratios with baleen and body length data from bowhead whales (Balaena mysticetus) to estimate whale age and explore anomalous years.* (3328426 Ph.D.), University of Washington, Ann Arbor.

Malinowski, C. R., & Herzing, D. L. (2015). Prey use and nutritional differences between reproductive states and age classes in Atlantic spotted dolphins (*Stenella frontalis*) in the Bahamas. *Marine Mammal Science, 31*(4), 1471-1493. doi: 10.1111/mms.12238.

Manlik, O., McDonald, J. A., Mann, J., Raudino, H. C., Bejder, L., Krützen, M., & Sherwin, W. B. (2016). The relative importance of reproduction and survival for the conservation of two dolphin populations. *Ecology and Evolution, 6*(11), 3496-3512. doi: 10.1002/ece3.2130.

Mann, J., Connor, R.C., Barre, L.M., & Heithaus, M. (1999). Female reproductive success in the bottlenose dolphins (*Tursiops sp.*): life history, habitat, provisioning, and group-size effects. *Behavioral Ecology, 11*(2), 210-219. doi: 10.1093/beheco/11.2.210.

Mattson, M. C., Mullin, K. D., Ingram, G. W., & Hoggard, W. (2006). Age structure and growth of the bottlenose dolphin (tursiops truncatus) from strandings in the Mississippi sound region of the north-central Gulf of Mexico from 1986 to 2003. *Marine Mammal Science, 22(3), 654-666*. doi: 10.1111/j.1748-7692.2006.00057.x.

Mazerolle, M.J. (2015). AICcmodavg: Model selection and multimodel inference based on (Q)AIC(c). R Package version 2.0-3.

McCluskey, S. M., Bejder, L., & Loneragan, N. R. (2016). Dolphin prey availability and calorific value in an estuarine and coastal environment. *Frontiers in Marine Science, 3*(30). doi: 10.3389/fmars.2016.00030.

McFee, W. E., Adams, J. D., Fair, P. A., & Bossart, G. D. (2012). Age distribution and growth of two bottlenose dolphin (*Tursiops truncatus*) populations from capture-release studies in the southeastern United States. *Aquatic Mammals, 38*(1), 17-30.

McFee, W. E., Schwacke, J. H., Stolen, M. K., Mullin, K. D., & Schwacke, L. H. (2010). Investigation of growth phases for bottlenose dolphins using a Bayesian modeling approach. *Marine Mammal Science, 26(1), 67-85*. doi: 10.1111/j.1748-7692.2009.00306.x.

Mead, J.G., & Potter, C.W. (1990). *Natural history of bottlenose dolphins along the central Atlantic coast of the United States.* In: Leatherwood, S., & Reeves, R.R. *The bottlenose dolphin* (65-195). New York, NY: Academic Press.

Meise, K., Mueller, B., Zein, B., & Trillmich, F. (2014). Applicability of single-camera photogrammetry to determine body dimensions of Pinnipeds: Galapagos sea lions as an example. *PLoS ONE, 9*(7). doi: 10.1371/journal.pone.0101197.

Mendez, M., Jefferson, T. A., Kolokotronis, S.O., Krützen, M., Parra, G. J., Collins, T., & Rosenbaum, H. C. (2013). Integrating multiple lines of evidence to better understand the evolutionary divergence of humpback dolphins along their entire distribution range: a new dolphin species in Australian waters? *Molecular Ecology, 22*(23), 5936-5948. doi: 10.1111/mec.12535.

Mirman, D. (2016). Growth Curve Analysis and Visualization using R. 63. CRC Press.

Mocklin, J. A., Rugh, D. J., Koski, W. R., & Lawrence-Slavas, N. (2010). Comparison of land-based vs. floating calibration targets used in aerial photogrammetric measurements of whale lengths. *Marine Mammal Science, 26*(4), 969-976. doi: 10.1111/j.1748-7692.2010.00389.x.

Monteiro-Filho, E. L. d. A., Monteiro, L. R., & dos Reis, S. F. (2002). Skull shape and size divergence in dolphins of the genus Sotalia: a tridimensional morphometric analysis. *Journal of Mammalogy, 83*(1), 125-134. doi: 10.1644/1545-1542(2002)083<0125:ssasdi>2.0.

Morris, W., Doak, D., Groom, M., Kareiva, P., Fieberg, J., Gerber, L., Murphy, P., & Thompson, D. (1999). *A practical handbook for population viability analysis* (1-3). Virginia, USA: The Nature Conservancy.

Morteo, E., Axayacati, R.O., Morteo, R., & Weller, D.W. (2017). Phenotypic variation in dorsal fin morphology of coastal bottlenose dolphins (*Tursiops truncatus*) off Mexico. *PeerJ Preprints, 4.* doi: https://doi.org/10.7287/peerj.preprints.2827v4.

Mumby, H. S., Chapman, S. N., Crawley, J. A. H., Mar, K. U., Htut, W., Thura Soe, A., & Lummaa, V. (2015). Distinguishing between determinate and indeterminate growth in a long-lived mammal. *BMC Evolutionary Biology, 15*(1), 214. doi: 10.1186/s12862-015-0487-x.

Murphy, S., & Rogan, E. (2006). External morphology of the short-beaked common dolphin, Delphinus delphis: growth, allometric relationships and sexual dimorphism. *Acta Zoologica, 87*(4), 315-329. doi: 10.1111/j.1463-6395.2006.00245.x.

Natsukari, Y. and Komine, N. (1992). Age and growth estimation of the European squid, *Loligo vulgaris*, based on statolith microstructure. *Journal of the Marine Biological Association. 72*, 271–280. doi: 10.1017/S0025315400037681.

Neuenhagen, C., García Hartmann, M., & Greven, H. (2007). Histology and morphometrics of testes of the white-sided dolphin (Lagenorhynchus acutus) in bycatch samples from the northeastern Atlantic. *Mammalian Biology - Zeitschrift für Säugetierkunde, 72*(5), 283-298. doi: 10.1016/j.mambio.2006.10.008.

Neuenhoff, R. (2009). Age, growth, and population dynamics of common bottlenose dolphins (*Tursiops truncatus*) along coastal Texas. *Wildlife and Fisheries Sciences, Texas A&M University*.

Nielsen, N. H., Garde, E., Heide-Jørgensen, M. P., Lockyer, C. H., Ditlevsen, S., Òlafsdóttir, D., & Hansen, S. H. (2013). Application of a novel method for age estimation of a baleen whale and a porpoise. *Marine Mammal Science, 29*(2), 1-23. doi: 10.1111/j.1748-7692.2012.00588.x.

O'Connell, C. P., & Leurs, G. (2016). A minimally invasive technique to assess several life-history characteristics of the endangered great hammerhead shark Sphyrna mokarran. *Journal of Fish Biology, 88*(3), 1257-1264. doi: 10.1111/jfb.12900.

Ogle, D.H. 2017. FSA: Fisheries Stock Analysis. R package version 0.8.12.

Olsen, M. T., Andersen, L. W., Dietz, R., Teilmann, J., Härkönen, T., & Siegismund, H. R. (2014). Integrating genetic data and population viability analyses for the identification of harbour seal (*Phoca vitulina*) populations and management units. *Molecular Ecology, 23*(4), 815-831. doi: 10.1111/mec.12644.

Paine, C. E. T., Marthews, T. R., Vogt, D. R., Purves, D., Rees, M., Hector, A., & Turnbull, L. A. (2012). How to fit nonlinear plant growth models and calculate growth rates: an update for ecologists. *Methods in Ecology and Evolution, 3*(2), 245-256. doi: 10.1111/j.2041-210X.2011.00155.x.

Panik, M. J. (2014). Fundamentals of population dynamics. *Growth curve modelling* (352-404): United States, John Wiley & Sons, Inc.

Pannella, G. (1971). Fish otoliths: daily growth layers and periodical patterns. *Science, 173*, 1124-1127. doi: 10.1126/science.173.4002.1124.

Pauly, D. (1979). Gill size and temperature as governing factors in fish growth: a generalization of von Bertlanffy's growth formula. Berichte Institut Meereskunde, Christian-Albrechts Universitaet, *63.*

Payne R, Brazier O, Dorsey E, Perkins J, Rowntree V, Titus A. (1983). External features in southern right whales (*Eubalaena australis*) and their use in identifying individuals. In: Payne R. Communication and behaviour of whales (371-445). Boulder, Colorado: Westview Press.

Peltier, H., Dabin, W., Daniel, P., Van Canneyt, O., Dorémus, G., Huon, M., & Ridoux, V. (2012). The significance of stranding data as indicators of cetacean populations at sea: Modelling the drift of cetacean carcasses. *Ecological indicators, 18*, 278-290. doi: http://dx.doi.org/10.1016/j.ecolind.2011.11.014.

Perryman, W. L., & Lynn, M. S. (1993). Identification of geographic forms of common dolphin (*Delphinus delphis*) from aerial photogrammetry. *Marine Mammal Science, 9*. doi: 10.1111/j.1748-7692.1993.tb00438.x.

Piercy, A. N., Carlson, J. K., & Passerotti, M. S. (2010). Age and growth of the great hammerhead shark, *Sphyrna mokarran*, in the north-western Atlantic Ocean and Gulf of Mexico. *Marine and Freshwater Research, 61*(9), 992-998. doi: https://doi.org/10.1071/MF09227.

Pitman, R. L., Wayne, L. P., Don, L., & Erik, E. (2007). A dwarf form of killer whale in Antarctica. *Journal of Mammalogy, 88*(1), 43-48. doi: https://doi.org/10.1644/06-MAMM-A-118R1.1.

Pleskach, K., Hoang, W., Chu, M., & Halldorson, T. (2016). Use of mass spectrometry to measure aspartic acid racemization for ageing beluga whales. *Marine Mammal Science, 32*(4), 1370-1380. doi: 10.1111/mms.12347.

Polanowski, A. M., Robbins, J., Chandler, D., & Jarman, S. N. (2014). Epigenetic estimation of age in humpback whales. *Molecular Ecology Resources, 14*(5), 976-987. doi: 10.1111/1755-0998.12247.

Prince, E.D., Lee, D.L., Zweigel, J.R., & Brothers, E.D. (1991). Estimating age and growth of young Atlantic blue marlin from otolith microstructure. *National Oceanic and Atmospheric Administration, 89.*

Rasband, W.S. (1997). ImageJ, U. S. National institutes of health, Bethesda, Maryland, USA. URL: http://imagej.nih.gov/ij/.

Ratkowsky, D. A. (1983). Nonlinear regression modeling: a unified practical approach, 288. New York, NY: Marcel Dekker Inc.

Read, A. J., Wells, R. S., Hohn, A. A. & Scott, M. D. (1993). Patterns of growth in wild bottlenose dolphins, *Tursiops truncatus*. *Journal of Zoology*, *231*(1), 107–123. doi: 10.1111/j.1469-7998.1993.tb05356.x.

Ridgway, S.H., & Fenner, C.A. (1982). Weight-length relationships of wild-caught and captive Atlantic bottlenose dolphins. Journal of the American Veterinary Medical Association, *181*(11), 1310-1315.

Robeck, T. R., Willis, K., Scarpuzzi, M. R., & O'Brien, J. K. (2015). Comparisons of life-history parameters between free-ranging and captive killer whale (Orcinus orca) populations for application toward species management. *Journal of Mammalogy, 96*(5), 1055-1070. doi: 10.1093/jmammal/gyv113.

Rohner, C. A., Richardson, A. J., Prebble, C. E. M., Marshall, A. D., Bennett, M. B., Weeks, S. J., & Pierce, S. J. (2015). Laser photogrammetry improves size and demographic estimates for whale sharks. *PeerJ, 3,* e886. doi: 10.7717/peerj.886.

Rowe, L. E., & Dawson, S. M. (2008). Laser photogrammetry to determine dorsal fin size in a population of bottlenose dolphins from Doubtful Sound, New Zealand. *Australian Journal of Zoology, 56*, 239-248. doi: http://dx.doi.org/10.1071/ZO08051.

Salewski, V., & Watt, C. (2017). Bergmann's rule: a biophysiological rule examined in birds. *Oikos, 126*(2). doi: 10.1111/oik.0369.

Schnute, J., & Fournier, D. (1980). A new approach to length–frequency analysis: growth structure. *Canadian Journal of Fisheries and Aquatic Sciences, 37*(9), 1337-1351. doi: 10.1139/f80-172.

Secchi E.R., Danilewicz D., and Ott, P.H. (2003) Applying the phylogeographic concept to identify franciscana dolphin stocks: implications to meet management objectives. *Journal of Cetacean Research and Management, 5*.

Siebert, U., Gilles, A., Lucke, K., Ludwig, M., Benke, H., Kock, K.H., & Scheidat, M. (2006). A decade of harbour porpoise occurrence in German waters—Analyses of aerial surveys, incidental sightings and strandings. *Journal of Sea Research, 56*(1), 65-80. doi: https://doi.org/10.1016/j.seares.2006.01.003.

Smith, H. C., Pollock, K., Waples, K., Bradley, S., & Bejder, L. (2013). Use of the robust design to estimate seasonal abundance and demographic parameters of a coastal bottlenose dolphin (*Tursiops aduncus*) population. *PLoS ONE, 8*. doi: 10.1371/journal.pone.0076574.

Smith, H., Frère, C., Kobryn, H., & Bejder, L. (2016). Dolphin sociality, distribution and calving as important behavioural patterns informing management. *Animal Conservation, 19*, 462-471. doi: 10.1111/acv.12263.

Sprogis, K. R., Pollock, K. H., Raudino, H. C., Allen, S. J., Kopps, A. M., Manlik, O., & Bejder, L. (2016). Sex-specific patterns in abundance, temporary emigration and survival of Indo-Pacific bottlenose dolphins (*Tursiops aduncus*) in coastal and estuarine waters. *Frontiers in Marine Science, 3*(12). doi: 10.3389/fmars.2016.00012.

Sprogis, K. R., Raudino, H. C., Rankin, R., MacLeod, C. D., & Bejder, L. (2016). Home range size of adult Indo-Pacific bottlenose dolphins (*Tursiops aduncus*) in a coastal and estuarine system is habitat and sex-specific. *Marine Mammal Science, 32(1), 287-308.* doi: 10.1111/mms.12260.

Sudarto, Lalu, X. C., Kosen, J. D., Tjakrawidjaja, A. H., Kusumah, R. V., Sadhotomo, B., & Paradis, E. (2010). Mitochondrial genomic divergence in coelacanths (Latimeria): slow rate of evolution or recent speciation? *Marine Biology, 157*(10), 2253-2262. doi: 10.1007/s00227-010-1492-7.

Sumich, J. L., & Show, I. T. (2011). Offshore migratory corridors and aerial photogrammetric body length comparisons of southbound Gray whales, *Eschrichtius robustus*, in the Southern California bight, 1988-1990. *Marine Fisheries Review, 73*(1), 28+.

Tofilski, A. (2000). Senescence and learning in honeybee *(Apis mellifera)* workers. *Acta Neurobiologiae Experientalis, 60*(1), 35-9.

Torres-Romero, E. J., Morales-Castilla, I., & Olalla-Tárraga, M. Á. (2016). Bergmann's rule in the oceans? Temperature strongly correlates with global interspecific patterns of body size in marine mammals. *Global Ecology and Biogeography, 25*(10), 1206-1215. doi: 10.1111/geb.12476.

Trabelsi, M., Maamouri, F., Quignard, J. P., Boussaïd, M., & Faure, E. (2004). Morphometric or morpho-anatomal and genetic investigations highlight allopatric speciation in western mediterranean lagoons within the Atherina lagunae species (*Teleostei, Atherinidae*). *Estuarine, Coastal and Shelf Science, 61*(4), 713-723. doi: http://dx.doi.org/10.1016/j.ecss.2004.07.011.

Vadopalas, B., Weidman, C., & Cronin, E. K. (2011). Validation of age estimation in geoduck clams using the bomb radiocarbon signal. *Journal of Shellfish Research, 30*(2), 303+.

van Rooij, J. M., & Videler, J. J. (1996). A simple field method for stereo-photographic length measurement of free-swimming fish: merits and constraints. *Journal of Experimental Marine Biology and Ecology, 195*(2), 237-249. doi: http://dx.doi.org/10.1016/0022-0981(95)00122-0.

Van Waerebeek, K. (1993). Geographic variation and sexual dimorphism in the skull of the dusky dolphin, *Lagenorhynchus obscurus* (Gray, 1828). *Fishery Bulletin, 91, 754-774.*

Vincenzi, S., Crivelli, A. J., Munch, S., Skaug, H. J., & Mangel, M. (2016). Trade-offs between accuracy and interpretability in von Bertalanffy random-effects models of growth. *Ecological Applications, 26*(5), 1535-1552. doi: 10.1890/15-1177.

Von Bertalanffy, L. (1938). A quantitative theory of organic growth (inquiries on growth laws. II). *Human Biology, 10*(2), 181-213. http://www.jstor.org/stable/41447359.

Wang, D., Atkinson, S., Hoover-Miller, A., Lee, S.-E., & Li, Q. X. (2007). Organochlorines in harbor seal (*Phoca vitulina*) tissues from the northern Gulf of Alaska. *Environmental Pollution, 146*. doi: http://dx.doi.org/10.1016/j.envpol.2006.01.050.

Webster, T., Dawson, S., & Slooten, E. (2010). A simple laser photogrammetry technique for measuring hector's dolphins (*Cephalorhynchus hectori*) in the field. *Marine Mammal Science, 26*(2), 296-308. doi: 10.1111/j.1748-7692.2009.00326.x.

Wells, R. S. (2009). Learning from nature: bottlenose dolphin care and husbandry. *Zoo Biology, 28*(6), 635-651. doi: 10.1002/zoo.20252.

Wijeyamohan S., Sivakumar V., Read B., Schmitt D., & Kumar S.K. (2012) A simple technique to estimate linear body measurements of elephants. *Current Science*, 102(1), 26.

Wursig, B., & Wursig, M. (1977). The photographic determination of group size, composition, and stability of coastal porpoises (*Tursiops truncates*). *Science, 198* (4318), 755-756. doi: 10.1126/science.198.4318.755.

Yuancai, L., Marques, C. P., & Macedo, F. W. (1997). Comparison of Schnute's and Bertalanffy-Richards' growth functions. *Forest Ecology and Management, 96*(3), 283-288. doi: http://dx.doi.org/10.1016/S0378-1127(96)03966-7.

Zambrano, L., Vega, E., Herrera M, L. G., Prado, E., & Reynoso, V. H. (2007). A population matrix model and population viability analysis to predict the fate of endangered species in highly managed water systems. *Animal Conservation, 10*(3), 297-303. doi: 10.1111/j.1469-1795.2007.00105.x.

Zelditch, M. L., Swiderski. D. L., Sheets, D.H., & Fink, W.L. (2004). Geometric morphometrics for biologists. Ontario, Burlington: Elsevier Science.

Zuk, M. (1987). Age determination of adult field crickets: methodology and field applications. *Canadian Journal of Zoology, 65*(6), 1564-1566. doi: 10.1139/z87-242.